Bose-Einstein condensation under the cubic-quintic Gross-Pitaevskii equation in radial domains

Ellen K. Luckins and Robert A. Van Gorder*

Mathematical Institute, University of Oxford, Andrew Wiles Building, Radcliffe Observatory Quarter, Woodstock Road, Oxford, OX2 6GG, United Kingdom

**Robert.VanGorder@maths.ox.ac.uk*

Abstract

We study stationary and quasi-stationary solutions for the cubic-quintic Gross-Pitaevskii equation modeling Bose-Einstein condensates (BECs) in one, two, and three spatial dimensions under the assumption of radial symmetry with the BEC dynamics influenced by a confining potential. We consider both repulsive and attractive cubic interactions - corresponding respectively to repulsive and attractive two-body interactions - under similar frameworks in order to deduce the effects of the potentials in each case. We also carefully consider the role played by the quintic nonlinearity (modeling the strength of inter-atomic coupling) in modifying the solutions arising due to a purely cubic interaction term. In one spatial dimension, we obtain a variety of exact solutions in the zero-potential limit (including new periodic solutions which generalize known soliton solutions) as well as perturbation solutions for small amplitude confining potentials. For more general forms of the confining potential, we rely on numerical simulations, but these agree with the analytical results when the latter are valid. We also consider the limit where the quintic term dominates the cubic term (with such a limit relevant in the study of a Tonks-Girardeau gas). Under the assumption of radial symmetry, we also consider cylindrical (or, cigar-shaped) and spherical BECs. We consider the nonperturbative regime where either the potential or the amplitude of the solutions is large, obtaining various qualitative analytical results. When the kinetic energy term is small (relative to the nonlinearity and the confining potential), we recover the expected Thomas-Fermi approximation for the stationary solutions. Numerical simulations, under a variety of external confining potentials, are then used to understand the role these potentials play on the BEC solution structure for both the attractive and repulsive regimes. This assortment of analytical and numerical results allows us to better understand the structure of BECs modeled via cubic-quintic Gross-Pitaevskii equation under confining potentials with radial symmetry. Some of the results are natural extensions of those for the cubic Gross-Pitaevskii equation, while others appear new.

Keywords: Gross-Pitaevskii equation, Bose-Einstein condensates, cubic-quintic nonlinearity, inter-atomic coupling, confining potential

---

1. Introduction

A Bose-Einstein Condensate (BEC), a state of matter consisting of a dilute gas of bosons cooled to temperatures very close to absolute zero, was originally hypothesised by Bose and Einstein in 1924, although the first BEC was only produced experimentally in 1995, winning the researchers Cornell, Ketterle and Wieman a Nobel Prize [1, 2]. A BEC consists of a gas of dilute boson particles, cooled to a critical temperature near absolute zero, so that the atoms condense down into their lowest energy state. BECs are studied because they can be made to exhibit quantum phenomena on a macroscopic scale, showing behaviours such as interference and diffraction, which we would only normally expect to see in much smaller particles such as photons and electrons.

Quantum vortices have been observed in BECs [3], and the mathematics of which is discussed in [4]. Solutions of the model are found under some simplification in [4] (by separating time-scales) to obtain the vortex solutions. BECs also exhibit a range of other macroscopic quantum phenomena, such as diffraction through a standing light wave, properties of which are studied in [5]. Standing light wave BEC traps are also used in the study of quantum logic [6], and phase coherence [7].

By modelling all atoms to be in the same, lowest quantum energy state, the whole collection of BEC particles may be described through just one complex scalar function, the *macroscopic wavefunction*. The interaction between BEC particles is then seen through a "self-interaction" of the macroscopic wavefunction, manifesting as a nonlinear term in the Schrödinger equation for the macroscopic wavefunction. The nonlinear Schrödinger equation (NLSE) for macroscopic wavenumber $\Psi(\boldsymbol{x}, t)$ (a function of space $\boldsymbol{x}$ and time t) is the Gross-Pitaevskiii equation:

$$i\hbar\frac{\partial\Psi}{\partial t} = \Big(- \frac{\hbar^2}{2m}\nabla^2 + V(\boldsymbol{x}, t) + f(|\Psi|^2)\Big)\Psi\,. \tag{1}$$

Here ∇^2 is the Laplacian operator, $\hbar$ is the reduced Planck constant, and m is a constant with units of mass. The function f gives the form of the nonlinear term representing the interaction between the BEC particles, and is a function of the density $|\Psi|^2$. We have also included an extra term $V(\boldsymbol{x}, t)\Psi$, which describes the interaction of the BEC with an external potential function imposed on the system. For instance if $V = 0$ there is no constraint on the condensate, or we may choose V to model a trap, confining the condensate to some region of space.

The mean-field approach by which this model may be derived was first used by Bogoliubov in 1947. It may also be derived rigorously from the complicated many-body problem as in [8] and [9], in the limit as the number of BEC particles approaches infinity. However, a general NLSE may also be derived from the first principles of classical field theory and classical mechanics, independent of the postulates of quantum mechanics[10].

When f in (1) is taken to be linear, we have the cubic Gross-Pitaevskiii equation (cGPE)

$$i\hbar\frac{\partial\Psi}{\partial t} = \Big(- \frac{\hbar^2}{2m}\nabla^2 + V(\boldsymbol{x}) + g|\Psi|^2\Big)\Psi \tag{2}$$

for some constant g (the sign of which describes whether interaction between BEC particles is attractive or repulsive). This is not always the best choice of nonlinearity. In certain specific situations it is more accurate to use a quintic, or cubic-quintic nonlinearity instead (we say more on this later). The GPE has also been studied with other forms of the nonlinearity, including non-polynomial forms, for instance in [11]. While these non-polynomial nonlinearities may be more accurate models in specific geometries, polynomial forms are still often used.

The cubic nonlinearity in the GPE (2) models BEC behaviour very well in many contexts, and it has consequently been well studied. As well as looking at the general solution of (2) for arbitrary potential as a perturbation about these zero-potential solutions, [12, 13, 14, 15] also consider both numerical and analytical solutions of the cGPE under some specific physically relevant potential functions. Earlier, [16] found a new family of exact stationary solutions in the situation of a repulsive BEC trapped in a standing light wave, which is modelled by a Jacobi elliptic function potential. Unlike [12, 13, 14, 15], [16] required no assumption that the potential was small, but their method only works for this specific potential, lacking the generality of [12, 13, 14, 15]. Other exact analytical solutions of the stationary equation have been found for other specific potentials, including the Kronig-Penney potential, solved in [17].

Other approaches reduce the full time-dependent cGPE to an ODE in different ways, as discussed in Section 4 of the review article [18]. Such methods include "variational approximation" (as it is described in [18]) which is widely used, and is discussed in detail in [19]. There is also the "moment method" used for instance in [20], and various similarity solution methods, used in [21] for instance. Other studies proceed by looking at the linear limit of the equation, and then considering the non-linear perturbations away from this limit, a method used for the cubic GPE in [22] for example. Equally, it is possible to examine the equation in the nonlinear limit. There is a large theory for the existence and stability of such solutions (for instance [23]), which may be found numerically as well as via analytical perturbation analyses ([24] gives a comprehensive review).

Motivated by the applications in mathematical physics such as BECs, research on solutions to cubic GP and NLS equations continues to be a topic of interest in the literature. New stationary solutions to the cubic NLS were recently studied in [25]. Stationary solutions of multicomponent NLS equations have also been considered [26]. A high-order conservative method for solving NLS and GP equations with time-varying coefficients used in modeling certain BECs was presented in [27]. Delayed collapse of BEC were considered in relation to anti-de Sitter gravity [28]. Analytical solutions of the 1D coupled Gross-Pitaevskiii equations governing the motion of spinor BECs were presented in [29].

Muryshev et al. [30] consider the dark soliton solutions to the cGPE in a long thin cylindrical geometry, in which the model may be reduced to 1D. [30] investigate the dynamic and thermodynamic stability of quasi-soliton structures, which dissipate over time unlike true solitons. Interestingly, the timescales over which the soliton structures dissipate is shown to be different for the 1D and 3D models considered, highlighting a potential inadequacy in the cGPE model. Instead of the cGPE, [30] derive a cqGPE (3) - a model involving cubic and quintic terms - as a better model than the cGPE in this geometry. The cubic-quintic Gross-Pitaevskiii equation (cqGPE) reads

$$i\hbar\frac{\partial\Psi}{\partial t} = \Big(-\frac{\hbar^2}{2m}\nabla^2 + V(\boldsymbol{x}) + g_1|\Psi|^2 + g_2|\Psi|^4\Big)\Psi\ , \tag{3}$$

and features an additional quintic self-interaction term. The signs of g_1 and g_2 describe whether interactions between two- and three-particle interactions, respectively, are repulsive or attractive. The cqGPE may be derived from the cGPE in the quasi-1D situation of BEC particles trapped in a long thin cigar-shaped tube in [30], or by altering the form assumed of the self-interaction to allow for three-particle as well as two-particle interactions. Köhler [31] explicitly derives the three-body interaction term for dilute BECs, which gives the extra quintic term in this model. The coefficient g_2 of the quintic term is also explicitly found in [31] in terms of material-specific parameters, using microscopic theory. Therefore, in situations where this quintic coefficient is sufficiently large (i.e., for particular types of BEC) we are justified in including the quintic term in the GPE. The cqGPE has been discussed as a better model than the cGPE if the BEC particles interact in such a way that three-particle interaction is as important as two-body interaction, as described in [18].

In some situations, a purely quintic model (without the cubic term, so $g_1 = 0$ in (3)) is most accurate. As explained in Sec. 3.5 of [18], the above discussion for cubic and cubic-quintic models implicitly assumed the interaction between the atoms was relatively weak. However, in the opposite limit, when there is moderate or strong inter-atomic coupling, models with only a quintic term in the self-interaction have been proposed, for instance for one and two dimensional geometries in [32]. A condensate with this strong inter-atomic coupling is known as a Tonks-Girardeau gas.

There have been attempts to find relevant solutions of the quintic and quintic-cubic models (qGPE and cqGPE respectively). Some specific stationary solutions of the purely quintic equation are studied in [32]. Tang and Shukla [33] find exact stationary solutions of the cqGPE under specific external potentials by allowing the coefficients of the cubic and quintic terms to be functions of space. These coefficients are then chosen to match the potential so that the solutions are possible, essentially reverse-engineering the solutions for the specific potentials used. A similar method of "nonlinearity management" is often used in the study of self-similar solutions such as in [34] and [35], with the coefficients g_1 and g_2 depending on both time and space. If these parameters depend on space or time in a very particular way, then similarity solutions may be possible for the cqGPE [36].

Other studies examining similarity solutions include [37], which employs a rigorous similarity solution method to find solutions of the 3D, spherically symmetric cqGPE in the case of a constant potential. Again, this requires certain conditions on the self-interaction and background potential terms. In fact, almost all of the solutions found require the coefficient of the cubic term to be zero. [38] study the purely quintic GPE with the potential dependent on both space and time, and similar time-independent studies are undertaken in the cubic-quintic and quintic cases in [39] and [33]. The form of these similarity solutions again requires a dependence between the background potential and the coefficient of the quintic term, which is also dependent on both space and time. In the case where this coefficient is in fact constant, it is possible to construct a solution under the harmonic potential, and some other physically relevant potentials. In [39], the authors study periodic potentials, again using similarity solutions and perturbation techniques. Solutions to the purely quintic GPE have been given on the unit circle [40]. Restricting to a finite domain gives a rather different problem to the infinite domain case, but it allows the authors to build a rigorous general theory. They consider no external potential.

Despite these studies, there has not been a systematic study of BEC under the cqGPE for various confining potentials. In this paper, we shall therefore study stationary and quasi-stationary solutions for the cubic-quintic Gross-Pitaevskii equation modeling Bose-Einstein condensates (BECs) in one, two, and three spatial dimensions with the BEC dynamics influenced by a confining potential. Geometrically, we shall restrict our attention to radially symmetric solutions when considering dynamics in $\mathbb{R}^d$ for $d > 1$. Repulsive and attractive cubic interactions, corresponding respectively to repulsive and attractive two-body interactions, are both considered. We also carefully consider the role played by the quintic nonlinearity in modifying the solutions arising due to a purely cubic interaction term. The cubic interaction term models two-body interactions, while the quintic term models the strength of inter-atomic coupling, and the balance of these terms with the confining potential will effectively drive the dynamics.

We shall consider a systematic study of stationary and quasi-stationary solutions to the cqGPE (3) for various confining potentials, akin to what was done in [12, 13, 14, 15] for the cGPE. The rest of the paper is organised as follows. In Section 2 we obtain the equations governing the dynamics of stationary solutions for (3). For restrictive assumptions on the confining potentials we are able to obtain exact solutions, including periodic solutions which generalize exact soliton solutions from the literature, and these are given in Section 3. Some of the exact solutions appear to be new. These solutions also generalize periodic solutions found for the cGPE [16] to the cqGPE model. For small confining potentials, we are also able to give analytical results via a perturbation method. In Section 4 we focus on the qGPE, again obtaining exact solutions. We are also able to obtain exact solutions under the assumption of a self-similarity assumption (rather than stationary solutions), which, again, appear new. While solutions for higher spatial dimensions than one are harder to come by, we give some analytical results along these lines in Section 5. For instance, we consider the nonperturbative regime where either the potential or the amplitude of the solutions is large, obtaining various qualitative analytical results. When the kinetic energy term is small (relative to the nonlinearity and the confining potential), we recover the expected Thomas-Fermi approximation for the stationary solutions. For stronger confining potentials taking arbitrary forms, we resort to numerical simulations, and we do this in Section 6. In particular, we fix either attractive and repulsive two-body interactions, and consider a variety of confining potentials (taking motivation in our selection from specific confining potentials used in the literature), in order to determine the role of the confining potential on the structure of the obtained BEC wave function. Furthermore, we vary the strength of the quintic nonlinearity, in order to see how a change in the balance between the cubic and quintic self-interaction terms will modify the solution structure. We also consider the limit where the quintic term dominates, which corresponds, for instance, to the regime with strong inter-atomic coupling. We discuss the results in Section 7.

2. Stationary Solutions

We now restrict to certain solution forms of the cqGPE, which reduces the equation to depend on space only. We will primarily consider stationary solutions of (3) of the form $\Psi(\boldsymbol{x},t) = ae^{ibt}\psi(\boldsymbol{x})$, for some real constants a and b. We also assume $\psi(\boldsymbol{x})$ is real-valued, although in principle we can consider this function as complex valued if we wish to have spatial terms in the phase. Substituting this into (3) and cancelling common factors, we obtain a stationary equation for ψ

$$-b\hbar\psi = -\frac{\hbar^2}{2m}\nabla^2\psi + g_1 a^2|\psi|^2\psi + g_2 a^4|\psi|^4\psi + V\psi \; . \tag{4}$$

We may fix a and b to balance terms. We choose to balance the left side of (4) with the first term on the right, and so obtain either $b = \frac{\hbar}{2m}$ or $b = -\frac{\hbar}{2m}$. In order to find bounded (and so physically relevant) solutions, we take $\mathrm{sgn}(b) = -\,\mathrm{sgn}(g_1)$. With this, (4) reduces to

$$\nabla^2\psi = G_1\psi^3 + G_2\psi^5 + \big(U(\boldsymbol{x}) - \mathrm{sgn}(G_1)\big)\psi \; , \tag{5}$$

where $G_1 = \frac{2mg_1a^2}{\hbar^2}$, $G_2 = \frac{2mg_2a^4}{\hbar^2}$ and $U(\boldsymbol{x}) = \frac{2m}{\hbar}V(\boldsymbol{x})$. We have also assumed that ψ is real, and so we removed the modulus signs. Notice that since a is real, $\mathrm{sgn}(g_1) = \mathrm{sgn}(G_1)$ and $\mathrm{sgn}(g_2) = \mathrm{sgn}(G_2)$.

We may also fix the modulus of G_1 or G_2 by specifying a. For instance if $a^2 = \frac{\hbar^2}{2m|g_1|}$ then $|G_1| = 1$. This also fixes $G_2 = \frac{g_2\hbar^2}{2m|g_1|^2}$. In the following sections we will seek solutions of (5) for various choices of G_1, G_2 and potential $U(\boldsymbol{x})$.

In one spatial dimension, the stationary cqGPE is:

$$\psi''(x) = G_1\psi^3(x) + G_2\psi^5(x) + \big(U(x) - \mathrm{sgn}(G_1)\big)\psi(x), \tag{6}$$

where $\psi''(x) = \frac{d^2\psi}{dx^2}$. In the case where there is no external potential (i.e.: $U(x) = 0$), we can find exact soliton and periodic solutions of (6). These quasi-soliton solutions are quoted regularly in the literature, for instance in [35] and [41], and are the analogues in the cubic-quintic case of the bright and dark soliton solutions of the cqGPE used in [12, 13].

If we consider a 2D geometry, in plane-polar coordinates (r,θ) the cqGPE (5) becomes

$$\frac{1}{r}\frac{\partial}{\partial r}\Big(r\frac{\partial\psi}{\partial r}\Big) + \frac{1}{r^2}\frac{\partial^2\psi}{\partial\theta^2} = G_1\psi^3 + G_2\psi^5 + \big(U(\boldsymbol{x}) - \mathrm{sgn}(G_1)\big)\psi. \tag{7}$$

For simplicity we consider a radially symmetric situation, so $\psi = \psi(r)$, and $U(r)$ are independent of θ. Then, expanding the r-derivative, (7) reduces to

$$\psi''(r) + \frac{1}{r}\psi'(r) = G_1\psi^3 + G_2\psi^5 + \Big(U(r) - \mathrm{sgn}(G_1)\Big)\psi\ , \tag{8}$$

where prime represents differentiation with respect to r. This will result in a cylindrical or "cigar-shaped" BEC.

We also consider a 3D geometry using spherical coordinates (r, θ, ϕ). In these coordinates the cqGPE (5) is

$$\frac{1}{r^2}\frac{\partial}{\partial r}\Big(r^2\frac{\partial\psi}{\partial r}\Big) + \frac{1}{r^2\sin\theta}\frac{\partial}{\partial\theta}\Big(\sin\theta\frac{\partial\psi}{\partial\theta}\Big) + \frac{1}{r^2\sin^2\theta}\frac{\partial^2\psi}{\partial\phi^2} = G_1\psi^3 + G_2\psi^5 + \Big(U(\boldsymbol{x}) - \mathrm{sgn}(G_1)\Big)\psi\ . \tag{9}$$

As in the 2D case, we will consider only radially symmetric situations, so that $\psi(r)$ and $U(r)$ are functions only of the radius r. The equation (9) then becomes

$$\psi''(r) + \frac{2}{r}\psi'(r) = G_1\psi^3 + G_2\psi^5 + \Big(U(r) - \mathrm{sgn}(G_1)\Big)\psi\ , \tag{10}$$

where prime represents differentiation with respect to r. This will result in a spherical BEC. Notice that this equation is very similar to (8), only with a different coefficient of the first derivative. The difference here will result in increased damping of the 3D solution relative to the 2D solution. The 2D solutions will scale with $r^{-1/2}$ while the 3D solutions will scale with r^{-1} for large r, as we shall later discuss.

The radial ODE for each case can be written as

$$\psi''(r) + \frac{d-1}{r}\psi'(r) = G_1\psi^3 + G_2\psi^5 + \Big(U(r) - \mathrm{sgn}(G_1)\Big)\psi\ , \tag{11}$$

where $d = 1, 2, 3$ is the dimension of the space. When $d = 1$ there do exist exact solutions for $U(r) \equiv 0$, and even for non-zero potentials, 1D cqGPE solutions can be explored analytically as well as numerically in a manner similar to [12, 13]. However, for $d = 2, 3$, the zero-potential equation is no longer integrable and so in general exact solutions do not exist for the cqGPE for $d = 2, 3$. Therefore, perturbation due to small potentials about a given exact solution is not possible in this case. Alternatively, one could assume both small amplitude and small potential, and carry out the perturbation analysis treating amplitude and potential jointly small in the same parameter. Unlike in the cGPE case, however, for the cqGPE, this type of analysis will push the quintic contribution off the second order corrections, meaning that the cubic term will dominate and results similar to those for the cGPE would be obtained. We shall therefore resort to numerical simulations, in order to study solutions to (11).

Will shall find numerical solutions for the stationary radial cqGPE (11) when an external potential $U(r)$ (depending only on the radius) is applied. We will look at the effects of a variety of specific potentials which are of physical relevance, the same as those used in [12, 13, 14, 15], in order to provide comparison between the cubic and cubic-quintic models.

3. Analytical results for 1D solutions under cubic-quintic nonlinearity

We shall first direct our attention to analytical solutions, including exact solutions, for the 1D case. Some of the solutions we report are new, and effectively generalize known solutions for the cGPE.

3.1. 1D attractive two-body interactions

Consider $G_1 < 0$. If there is no external potential, $U(x) = 0$, there exists an exact bright soliton solution to (6). Adapted from that used in [41], for arbitrary negative coefficients G_1 and G_2,

$$\psi(x) = \frac{2}{\sqrt{A\cosh(2x) - G_1}}, \tag{12}$$

where $A = \sqrt{G_1^2 - \frac{16}{3}G_2}$ is a real positive constant, is a solution of the zero-potential equation

$$\psi''(x) = G_1\psi^3(x) + G_2\psi^5(x) + \psi(x). \tag{13}$$

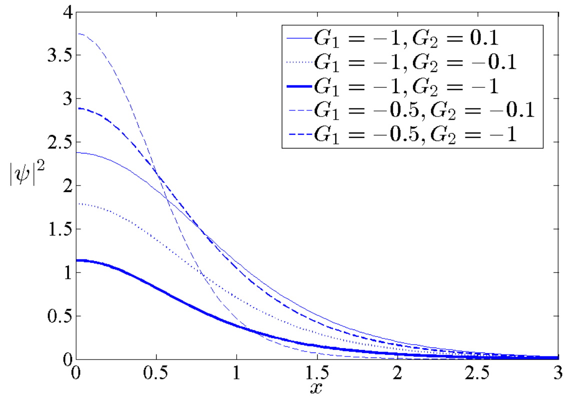

Figure 1: Exact bright soliton solutions (12) for various values of G_1 and G_2. For greater G_2 the amplitude of the soliton increases, while increasing G_1 increases both the amplitude, and rate of decay.

Note that (12) is also a solution of (13) when $G_1 < 0$ and $G_2 > 0$, so long as $\frac{3G_1^2}{16} > G_2$. This solution is plotted for various values of G_1 and G_2 in Fig. 1.

The soliton solutions are not the most general form of exact solution, however, and actually require very particular parameter constraints. In the case of the cGPE, there exist families of solutions involving Jacobi elliptic functions [12, 13], and the solitons correspond to fixing the elliptic index at a specific value. We shall now show that a similar property holds for the cqGPE. The exact solutions we obtain appear to be new for the cqGPE.

Multiplying (13) by $\psi'(x)$ we see that each side is a total derivative:

$$\frac{d}{dx}\left[\frac{(\psi'(x))^2}{2}\right] = \frac{d}{dx}\left[\frac{G_1}{4}\psi^4(x) + \frac{G_2}{6}\psi^6(x) + \frac{1}{2}\psi^2(x)\right],$$

and so integrating and separating variables, we find the implicit solution:

$$\pm x = \int_{\psi(0)}^{\psi(x)} \frac{d\varphi}{\sqrt{\frac{G_1}{2}\varphi^4(x) + \frac{G_2}{3}\varphi^6(x) + \varphi^2(x) + C}}\,. \tag{14}$$

The elliptic form of the integral motivates a search for a periodic solution. By comparison with literature such as [42], the form of the soliton solution (12), and the use of Jacobi elliptic functions in the analysis of the cGPE in [12, 13], we look for periodic solutions of the form

$$\psi(x) = \frac{A\,\mathrm{cn}(ax,k)}{\sqrt{1 + \mathrm{cn}(ax,k)^2}}\,, \tag{15}$$

where $\mathrm{cn}(ax,k)$ is a Jacobi elliptic function, and A, a, and k are constants (depending on G_1 and G_2) to be found. Substituting (15) into (13), we see such a solution exists subject to three conditions on A, a, and k, which may be solved to obtain

$$a^2 = -\frac{1}{14}(16 + 5G_1A^2)\,, \quad k^2 = \frac{2(5 + 2G_1A^2)}{16 + 5G_1A^2}\,, \quad \text{and} \quad A = \pm\sqrt{\frac{-9G_1 \pm \sqrt{81G_1^2 - 336G_2}}{14G_2}}\,. \tag{16}$$

We need the amplitude A to be real and positive and the scaling a to be real. For a to be real, we require $G_1 < -\frac{16}{5A^2}$. If $G_2 < 0$, then since $G_1 < 0$, we take

$$A = \sqrt{\frac{-9G_1 - \sqrt{81G_1^2 - 336G_2}}{14G_2}}\,,$$

while if $G_2 > 0$, A is only real if $0 < G_2 < \frac{27}{112}G_1^2$, in which case either of the two roots

$$A = \sqrt{\frac{-9G_1 \pm \sqrt{81G_1^2 - 336G_2}}{14G_2}} \, ,$$

may be chosen. We can then compute $a(G_1, G_2)$ and $k(G_1, G_2)$ using the relevant expression for A in (16), and so have fully determined a periodic solution of the form (15).

Suppose now that the external potential is $U(x) = \delta$ for some small constant $|\delta| << 1$. With such a potential, equation (6) may be rescaled to the same form as the zero-potential equation, i.e.: with $U(x) = 0$. This allows us to view solutions of (6) with a constant potential function merely as scaled solutions of the zero-potential equation examined in the previous section. We therefore include no further analysis of constant-potential solutions. Although we include this argument in the $G_1 < 0$ section, the analysis is general, holding for all choices of G_1, G_2.

We change variables by defining

$$\psi(x) = \frac{\phi(X)}{|\delta - \mathrm{sgn}(G_1)|} \quad \text{where} \quad X = \sqrt{|\delta - \mathrm{sgn}(G_1)|}x \, ,$$

so that (6) becomes

$$\phi''(X) = \hat{G}_1\phi^3(X) + \hat{G}_2\phi^5(X) - \mathrm{sgn}(\hat{G}_1)\phi(X) \, ,$$

where $\hat{G}_1 = G_1|\delta - \mathrm{sgn}(G_1)|^{-3}$ and $\hat{G}_2 = G_2|\delta - \mathrm{sgn}(G_1)|^{-5}$. Notice that $\mathrm{sgn}(G_1) = \mathrm{sgn}(\hat{G}_1)$ and $\mathrm{sgn}(G_2) = \mathrm{sgn}(\hat{G}_2)$, and we have used the fact that $\delta << 1$ to find the coefficient of the final term. Hence the constant-potential equation may be rescaled to a zero-potential equation, retaining coefficients with the same sign as in the original equation, and the bright soliton or periodic solutions we obtained above can be used.

3.2. 1D repulsive two-body interactions

Consider $G_1 > 0$. With $U(x) = 0$, (6) is

$$\psi''(x) = G_1\psi^3(x) + G_2\psi^5(x) - \psi(x). \tag{17}$$

There exists a dark soliton solution of (17), namely:

$$\psi(x) = \frac{\sinh(Bx)}{\sqrt{A\sinh^2(Bx) + C}} \, , \tag{18}$$

where if we define $\tilde{G} = \sqrt{G_1^2 + 4G_2}$, then $A = \frac{G_1+\tilde{G}}{2}$, $B = \sqrt{\frac{\tilde{G}}{G_1+\tilde{G}}}$, and $C = \frac{1}{2}(\sqrt{1 + 6G_1 + 6\tilde{G}} - 1)$ are constants. This solution appears to be new, and generalizes the tanh-type dark soliton known in the literature for the case of purely cubic nonlinearity. Note that this is also a solution if $G_1 > 0$ and $-\frac{G_1^2}{4} < G_2 < 0$. Observe that

$$|\psi|^2 \to \frac{1}{A} = \frac{2}{G_1 + \sqrt{G_1^2 + 4G_2}}$$

as $x \to \pm\infty$.

Under $G_1 > 0$, an implicit solution of (6) exists, and takes the form

$$\pm x = \int_{\psi(0)}^{\psi(x)} \frac{d\varphi}{\sqrt{\frac{G_1}{2}\varphi^4(x) + \frac{G_2}{3}\varphi^6(x) - \varphi^2(x) + C}} \, , \tag{19}$$

which motivates a search for solutions of the form

$$\psi(x) = \frac{A\,\mathrm{sn}(ax, k)}{\sqrt{1 + \mathrm{sn}(ax, k)^2}} \, , \tag{20}$$

for A, a and k to be determined. Substituting (20) into (6) gives

$$a^2 = \frac{1}{14}(6 - G_1 A^2)\,, \quad k^2 = \frac{2(2G_1A^2 - 5)}{6 - G_1 A^2}\,, \quad \text{and} \quad A = \pm\sqrt{\frac{-9G_1 \pm \sqrt{81G_1^2 + 336G_2}}{14G_2}}\,. \tag{21}$$

As before, we require A real and positive and a real for this solution to be well-defined. For a to be real, we must require $0 < G_1 < \frac{6}{A^2}$, which defines a restriction on the size of G_1 in terms of G_2. If $G_2 > 0$, we therefore take

$$A = \sqrt{\frac{-9G_1 + \sqrt{81G_1^2 + 336G_2}}{14G_2}}\,,$$

and if $G_2 < 0$, A is only real if $G_2 > -\frac{27}{112}G_1^2$, in which case either of the two roots

$$A = \sqrt{\frac{-9G_1 \pm \sqrt{81G_1^2 + 336G_2}}{14G_2}}\,,$$

may be chosen. Then a and k are found by substitution into (21), fully determining the solution (20). Again, these generalised repulsive solutions for the cqGPE appear to be new.

3.3. 1D solutions under specific periodic potentials

Recall that [16] and others have considered elliptic function potentials for the cGPE, and obtain stationary solutions which are periodic. We shall now demonstrate exact periodic solutions for the cqGPE. The results of [16] rely on choosing a periodic potential which effectively induces a periodic solution to a cubic NLS equation. Their approach involves considering the potential to scale with the elliptic function, while the solution will scale as the square root of such a function. However, one may similarly define the potential to be the square of an elliptic function, in order to obtain a solution which itself scales an an elliptic function. It is this latter approach we shall use, as it is both more analytically tractable and results in a simpler solution form.

We shall always assume a potential is applied which takes the form

$$U(x) = U_0 + U_1(\mathrm{sn}(ax,k))^2 + U_2(\mathrm{sn}(ax,k))^4\,. \tag{22}$$

We shall consider three cases, corresponding to Jacobi elliptic sn, cn, and dn functions. First, the potential (22) induces a stationary solution of the form

$$\psi(x) = A\,\mathrm{sn}(ax,k) \tag{23}$$

provided that

$$U_0 = \mathrm{sgn}(G_1) - a^2(1+k^2)\,, \quad U_1 = 2a^2k^2 - G_1A^2\,, \quad U_2 = -G_2A^4\,. \tag{24}$$

Therefore, we can tune the potential (22) with parameters (24) in order to obtain a periodic sn type solution of the form (23).

Similarly, the potential (22) induces a stationary solution of the form

$$\psi(x) = A\,\mathrm{cn}(ax,k) \tag{25}$$

provided that the parameters are tuned like

$$U_0 = \mathrm{sgn}(G_1) - G_2A^4 - G_1A^2 - a^2\,, \quad U_1 = 2a^2k^2 + 2G_2A^4 + G_1A^2\,, \quad U_2 = -G_2A^4\,. \tag{26}$$

Finally, the potential (22) induces a stationary solution of the form

$$\psi(x) = A\,\mathrm{dn}(ax,k) \tag{27}$$

provided that the parameters are tuned like

$$U_0 = \mathrm{sgn}(G_1) - G_2A^4 - G_1A^2 - a^2k^2\,, \quad U_1 = 2a^2k^2 + 2G_2A^4k^2 + G_1A^2k^2\,, \quad U_2 = -G_2A^4k^4\,. \tag{28}$$

Therefore, we can tune a general potential involving a polynomial of even powers in the Jacobi elliptic function sn, in order to construct any periodic wave function solution give in terms of a Jacobi sn, cn, or dn elliptic function, as was previously done for the cGPE. These solutions appear to be new for the cqGPE.

3.4. Perturbations of 1D exact solutions under small yet arbitrary potentials

We suppose we have an exact solution for the zero-potential equation (6) with $U(x) = 0$, such as our soliton solutions (12) and (18). We analyse the effect of introducing a small potential on these solutions, and expect that the new solution under the potential will be close to the original zero-potential solution. We therefore perform a perturbation analysis similar to that used in [12, 13], although more general, on the equation

$$\psi''(x) = G_1\psi^3(x) + G_2\psi^5(x) + \Big(\epsilon U(x) - \mathrm{sgn}(G_1)\Big)\psi(x) \,, \tag{29}$$

where $\epsilon << 1$ is a small parameter. In fact, we will carry out the analysis for a more general equation of the form:

$$\psi''(x) = \sum_{k=1}^{n} \alpha_k \psi^k(x) + \epsilon U(x)\psi(x) \,, \tag{30}$$

for some finite natural number n, and constants α_k. The analysis for the cGPE given in [12, 13] is therefore the case $n = 3$, α_1 and α_3 non-zero, and $\alpha_2 = 0$, whereas for our cqGPE (29), we have $n = 5$, $\alpha_2 = \alpha_4 = 0$ and $\alpha_1 = -\,\mathrm{sgn}(G_1)$, $\alpha_3 = G_1$, and $\alpha_5 = G_2$.

We look for solutions to (30) of the form $\psi = \psi_0 + \epsilon\psi_1 + \epsilon^2\psi_2 + O(\epsilon^3)$, expanding in the small parameter ϵ. Substituting this into (30) we obtain

$$\psi_0''(x)+\epsilon\psi_1''(x)+\epsilon^2\psi_2''(x)+\cdots = \sum_{k=1}^{n}\alpha_k\Big(\psi_0(x)+\epsilon\psi_1(x)+\epsilon^2\psi_2(x)+\cdots\Big)^k + \epsilon U(x)\Big(\psi_0(x)+\epsilon\psi_1(x)+\epsilon^2\psi_2(x)+\cdots\Big) \,. \tag{31}$$

To leading order, this gives the zero-potential equation

$$\psi_0''(x) = \sum_{k=1}^{n}\alpha_k\psi_0^k(x) \,, \tag{32}$$

so that in our cubic-quintic case, ψ_0 satisfies the zero-potential equation, and so ψ_0 may be our soliton solution, or some other solution of the zero-potential equation. We assume ψ_0 solves (32).

At $O(\epsilon)$, (31) gives

$$\psi_1''(x) = \sum_{k=1}^{n} k\alpha_k\psi_0^{k-1}(x)\psi_1(x) + \psi_0(x)U(x) \,. \tag{33}$$

We will now solve (33) for $\psi_1(x)$ in terms of $U(x)$ and $\psi_0(x)$ which are known. Multiplying both sides of (33) by ψ_0' and then adding $\psi_0''\psi_1'$ to each side, gives

$$\frac{d}{dx}\Big[\psi_0'\psi_1'\Big] = \frac{d}{dx}\Big[\psi_1\Big(\sum_{k=1}^{n}\alpha_k\psi_0^k\Big)\Big] + \psi_0\psi_0' U \,.$$

Integrating with respect to x, we obtain

$$\psi_0'\psi_1' = \psi_1\Big(\sum_{k=1}^{n}\alpha_k\psi_0^k\Big) + \int_0^x \psi_0(\hat{x})\psi_0'(\hat{x})U(\hat{x})d\hat{x} \,,$$

where the constant of integration is zero since $\psi_1'(0) = 0$. Using (32) again, this is

$$(\psi_0')^2\frac{d}{dx}\Big[\frac{\psi_1}{\psi_0'}\Big] = \int_0^x \psi_0(\hat{x})\psi_0'(\hat{x})U(\hat{x})d\hat{x} \,.$$

We integrate once more, and gain an explicit expression for ψ_1:

$$\psi_1(x) = \int_0^x \frac{\psi_0'(x)}{(\psi_0'(x'))^2}\Big(\int_0^{x'}\psi_0(\hat{x})\psi_0'(\hat{x})U(\hat{x})d\hat{x}\Big)dx' \,, \tag{34}$$

where the constant of integration is zero since $\psi_1(0) = 0$.

We may extend this analysis to higher order corrections, by exploiting the fact that at j^{th} order in ϵ the right hand side of (31) is linear in ψ_j. In fact, the $O(\epsilon^j)$ equation always has the form

$$\psi_j''(x) = \Big(\sum_{k=1}^{n} k\alpha_k\psi_0^{k-1}(x)\Big)\psi_j(x) + W_j(x)\,,$$

for some function $W_j(x)$ which is a function of the lower order corrections $\psi_m(x)$ for $m < j$ and $U(x)$, and so is known. For example, in this form, $W_1(x) = \psi_0(x)U(x)$, and it is straightforward to see that at second order,

$$W_2(x) = \psi_1(x)U(x) + \sum_{k=1}^{n}\binom{k}{2}\alpha_k\psi_0^{k-2}(x)\psi_1^2(x).$$

We can then generalise the above argument, replacing ψ_1 with generic ψ_j for $j \geq 1$ to solve for $\psi_j(x)$ explicitly:

$$\psi_j(x) = \int_0^x \frac{\psi_0'(x)}{(\psi_0'(x'))^2}\Big(\int_0^{x'}\psi_0'(\hat{x})W_j(\hat{x})d\hat{x}\Big)dx'\,, \tag{35}$$

where we have also used $\psi_j(0) = \psi_j'(0) = 0$.

A perturbation solution can then be written

$$\psi(x) = \sum_{m=0}^{\infty}\psi_m(x)\epsilon^m = \int_0^x \frac{\psi_0'(x)}{(\psi_0'(y))^2}\left(\int_0^y \psi_0'(z)\sum_{j=0}^{\infty}\epsilon^j W_j(z)dz\right)dy\,. \tag{36}$$

While such a solution is of less practical use on its own when compared to the aforementioned exact solutions, it can be used in comparison with numerical solutions in the small ϵ regime, which is useful for validation of numerical solutions.

4. Analytical results for 1D solutions under purely quintic nonlinearity

As discussed in Section 1, there are situations in which it is most accurate to use only a quintic nonlinearity, rather than the cubic-quintic, with one example being a Tonks-Girardeau gas. In addition, in certain regimes the cubic-quintic GPE reduce to a purely quintic GPE at leading order. For instance, we may consider a coordinate transformation on the full time-dependent cubic-quintic GPE:

$$i\Psi_t = -\nabla^2\Psi + g_1|\Psi|^2\Psi + g_2|\Psi|^4\Psi + V(\boldsymbol{x},t)\Psi\,, \tag{37}$$

where $V(\boldsymbol{x},t)$ is the potential function. Here we have scaled the original cqGPE (3), which may be done by scaling the t-variable for instance, and altering the magnitude of g_1, g_2 and the potential V.

Suppose that the amplitude of the solution is large, so we scale $\Psi(\boldsymbol{x},t) = \Psi_0\varphi(\boldsymbol{x}',t')$, for $\Psi_0 >> 1$. If we take $\boldsymbol{x}' = \Psi_0^2\boldsymbol{x}$, $t' = \Psi_0^4 t$ (so we consider long time-scales and length-scales), and if the potential is small, scaling like $U(\boldsymbol{x}',t) = \Psi_0^{-4}V(\boldsymbol{x},t)$, then the equation (37) becomes:

$$i\varphi_{t'} = -\nabla'^2\varphi + \frac{g_1}{\Psi_0^2}|\varphi|^2\varphi + g_2|\varphi|^4\varphi + U(\boldsymbol{x}',t)\varphi\,,$$

and so to leading order in $\Psi_0^{-2} << 1$ we see that the equation reduces to the purely quintic GPE:

$$i\varphi_{t'} = -\nabla'^2\varphi + g_2|\varphi|^4\varphi + U(\boldsymbol{x}',t)\varphi\,.$$

We are therefore justified in studying the GPE with purely quintic nonlinearity:

$$i\frac{\partial\Psi}{\partial t} = \Big(-\nabla^2 + V(\boldsymbol{x},t) + g_2|\Psi|^4\Big)\Psi\,. \tag{38}$$

We shall demonstrate certain analytical solutions in this case. Note that the perturbation solutions in Section 2 still apply, as one would just need to set the α multiplying the cubic term to zero in all of those formulas, therefore we do not repeat it here.

4.1. Stationary solutions

Looking for stationary solutions $\Psi = ae^{ibt}\psi(\boldsymbol{x})$ for appropriate choices of a and b, as in Section 2, the stationary quintic equation is

$$\nabla^2\psi = G_2\psi^5 + \Big(U(\boldsymbol{x}) - \mathrm{sgn}(G_2)\Big)\psi\,. \tag{39}$$

We look at the 1D case, where the (39) reduces to the ODE

$$\psi''(x) = G_2\psi^5(x) + \Big(U(x) - \mathrm{sgn}(G_2)\Big)\psi(x)\,. \tag{40}$$

If $U(x)$ is zero, (40) has the same soliton and periodic solutions as the cubic-quintic equation, with $G_1 = 0$. Also, by the arguments in Section 2, these are also solutions after suitable scaling if $U(x)$ is a sufficiently small constant.

More explicitly, if $G_2 < 0$ then the zero-potential equation

$$\psi''(x) = G_2\psi^5(x) + \psi(x)$$

has a bright soliton solution

$$\psi(x) = \frac{\left(\frac{3}{-G_2}\right)^{1/4}}{\sqrt{\cosh(2x)}}\,,$$

and periodic solutions, such those found in Section 2.

If instead $G_2 > 0$, then the zero-potential equation

$$\psi''(x) = G_2\psi^5(x) - \psi(x)$$

has dark soliton solution

$$\psi(x) = \frac{\sinh(x)}{\sqrt{\sqrt{G_2}\sinh^2(x) + \frac{1}{2}\big(\sqrt{1 + 12\sqrt{G_2}} - 1\big)}}\,.$$

and periodic solutions as found in Section 2.

Since (40) is less complicated than the full cubic-quintic equation, we may also be able to find exact solutions for other specific forms of $U(x)$, although we do not explore this point further in this paper.

4.2. Quasi-stationary solutions obeying a self-similarity scaling

Rather than considering stationary solutions, another way to reduce the 1D (scaled) cqGPE (37) to an ODE is to assume a similarity solution, which give a quasi-stationary type of solutions within which time is scaled out of the problem in a way that utilises a self-similar variable involving space and time. In this section, we shall obtain what appear to be new exact solutions of this form for the qGPE.

Similarity solutions have been used in many studies, in the cubic, cubic-quintic, and quintic cases, for example in [43, 34, 21] While useful in certain cases, similarity solutions require very specific forms of the potential $V(x,t)$, and, if both cubic and quintic terms are included in the equation, they also require specific time-dependence of the coefficients $G_1(t)$ and $G_2(t)$, for instance in [34, 35]. Here we will only summarise the process, and find some simple self-similar solutions to the quintic GPE (38). Note that, for constant G_1 and G_2, it is simple to show that the cqGPE has no similarity solutions, which is why we do not consider such a case. It is for this reason that many studies consider "nonlinearity management" via non-autonomous coefficients $G_1(x,t)$ and $G_2(x,t)$, such as in [34, 35].

We look for solutions of (38), where $V = V(x,t)$ is a function of space and time, of the form $\Psi(x,t) = t^\alpha\Phi(\eta)$, where $\eta = xt^\beta$. Substituting into (38), we see that the only pair of parameters α and β which yield an equation depending only on the similarity variable η is $\alpha = -\frac{1}{4}, \beta = -\frac{1}{2}$. Furthermore, for such a solution to exist, the potential must have the form $V(x,t) = t^{-1}\mathcal{U}(\eta)$. In this case, (38) reduces to an ODE for $\Phi(\eta)$ given by

$$-\frac{i}{4}(\Phi + 2\eta\Phi') = -\Phi'' + G_2|\Phi|^4\Phi + \mathcal{U}\Phi\,, \tag{41}$$

where the primes denote differentiation with respect to η.

We look for complex valued solutions of (41) of the form $\Phi(\eta) = R(\eta)e^{i\theta(\eta)}$, so that, substituting this into (41) and separating real and imaginary parts, we have

$$\frac{1}{4}\Big(R + 2\eta R'\Big) = R\theta'' + 2R'\theta' \ , \tag{42}$$

$$\frac{1}{2}\eta R\theta' = -R'' + R(\theta')^2 + G_2R^5 + \mathcal{U}R \ . \tag{43}$$

Note that, multiplying through by R, (42) can be written as a total derivative,

$$\frac{d}{d\eta}\Big[R^2\theta' - \frac{\eta}{4}R^2\Big] = 0 \ ,$$

which implies

$$\theta(\eta) = \theta(0) + \frac{\eta^2}{8} + \int_0^\eta \frac{\theta'(0)R(0)^2}{R(\hat{\eta})^2}d\hat{\eta} \, . \tag{44}$$

With this, (43) becomes

$$R''(\eta) + \left(\frac{\eta^2}{16} - \mathcal{U}\right)R = G_2R^5 + \frac{\theta'(0)^2R(0)^4}{R^3} \ . \tag{45}$$

In order to obtain certain exact solutions, we consider the specific case when $\theta(0) = \theta'(0) = 0$. With this assumption, the ODE for R reduces to

$$R''(\eta) + \left(\frac{\eta^2}{16} - \mathcal{U}\right)R = G_2R^5 \ . \tag{46}$$

To make further progress toward finding exact solutions, we must specify the form of $\mathcal{U}(\eta)$. We shall consider three cases.

4.2.1. *Potential of the form* $\mathcal{U} = \frac{\eta^2}{16}$

First, if $\mathcal{U} = \frac{\eta^2}{16}$ then (46) is merely

$$R'' = G_2R^5 \ ,$$

which gives

$$(R')^2 = \frac{G_2}{3}R^6 + C \ ,$$

for some constant C. If $C \neq 0$ we would probably obtain a periodic solution. We will consider a similar situation later, so for now we take the special case with $C = 0$. Then, if $G_2 > 0$,

$$\frac{dR}{d\eta} = \pm\sqrt{\frac{G_2}{3}}R^3 \ ,$$

and so separating variables, we obtain

$$R^2 = \frac{R(0)^2}{1 \pm 2\sqrt{\frac{G_2}{3}}\eta R(0)^2} \ .$$

Taking the "plus" root to avoid solutions diverging for positive η, we see

$$R(\eta) = \frac{R(0)}{\sqrt{1 + 2\sqrt{\frac{G_2}{3}}\eta R(0)^2}} \ .$$

Returning to physical variables, the solution we have found is

$$\Psi(x,t) = \frac{t^{-1/4}R(0)}{\sqrt{1 + 2xt^{-1/2}\sqrt{\frac{G_2}{3}}R(0)^2}}\exp\left(\frac{ix^2}{8t}\right) ,$$

for any parameter $R(0) > 0$, where

$$U(x,t) = \left(\frac{x}{4t}\right)^2 \ .$$

4.2.2. Potential of the form $\mathcal{U} = \frac{\eta}{16} - \mathcal{U}_0$

Next, consider $\mathcal{U} = \frac{\eta}{16} - \mathcal{U}_0$ for a constant $\mathcal{U}_0 > 0$. Then (46) is

$$R'' + \mathcal{U}_0 R - G_2 R^5 = 0\,. \tag{47}$$

We look for periodic solutions to (47) of the form

$$R(\eta) = \frac{A\,\mathrm{cn}(a\eta, k)}{\sqrt{1 + \mathrm{cn}(a\eta, k)^2}}\,.$$

Substituting this into (47) gives conditions on the parameters a, k, and A. We obtain $k = \sqrt{\frac{5}{8}}$, $a^2 = \frac{8}{7}\mathcal{U}_0$, $A^4 = 2\frac{\mathcal{U}_0}{G_2}$, so that A is real if $\frac{\mathcal{U}_0}{G_2} > 0$ and a is real if $\mathcal{U}_0 > 0$. In that case our solution, in physical variables, is

$$\Psi(x,t) = \frac{\left(\frac{2\mathcal{U}_0}{G_2}\right)^{1/4} \mathrm{cn}\left(xt^{-1/2}\sqrt{\frac{8}{7}\mathcal{U}_0},\, \sqrt{\frac{5}{8}}\right)}{t^{1/4}\sqrt{1 + \mathrm{cn}\left(xt^{-1/2}\sqrt{\frac{8}{7}\mathcal{U}_0},\, \sqrt{\frac{5}{8}}\right)^2}} \exp\left(\frac{ix^2}{8t}\right), \tag{48}$$

when the potential is

$$U(x,t) = \left(\frac{x}{4t}\right)^2 - \frac{\mathcal{U}_0}{t}\,.$$

This solution is valid for $\mathcal{U}_0 > 0$ and $G_2 > 0$.

4.2.3. Composite elliptic potential

Consider now a potential

$$\mathcal{U} = \frac{\eta^2}{16} - \mathcal{U}_0 - \mathcal{U}_1(\mathrm{sn}(a\eta, k))^4\,.$$

This generalises the potentials used in [16] and others to the quasi-static or self-similar case. Here we have a harmonic part, a constant part, and a periodic part given by a Jacobi elliptic sn function. Eq. (46) is put into the form

$$R'' + \mathcal{U}_0 R + \mathcal{U}_1(\mathrm{sn}(a\eta, k))^4 R - G_2 R^5 = 0\,. \tag{49}$$

We shall assume that this potential induces a periodic solution of the form $R(\eta) = A\mathrm{sn}(a\eta, k)$. As earlier done in Section 2, we obtain necessary conditions on the parameters if we place this solution anzats into (49), obtaining $A = \left(\frac{\mathcal{U}_1}{G_2}\right)^{1/4}$, $a = \sqrt{\mathcal{U}_0}$, $k = \sqrt{\frac{\mathcal{U}_1}{\mathcal{U}_0}}$. Hence, the parameters of the solution and potential will need to synchronize in order for a solution to exist, and, further, the solution parameters will all depend on the remaining free parameters in the potential which measure the relative strength of each of the three terms in the potential. The amplitude will also scale with $G_2^{-1/4}$, meaning that the periodic waves will de-amplify as the intra-atomic coupling increases.

Therefore, a potential

$$U(x,t) = \left(\frac{x}{4t}\right)^2 - \frac{\mathcal{U}_0}{t} - \frac{\mathcal{U}_1}{t}\left(\mathrm{sn}\left(\sqrt{\frac{\mathcal{U}_0}{t}}x,\, \sqrt{\frac{\mathcal{U}_1}{\mathcal{U}_0}}\right)\right)^4 \tag{50}$$

induces a wavefunction

$$\Psi(x,t) = \left(\frac{\mathcal{U}_1}{G_2 t}\right)^{1/4} \mathrm{sn}\left(\sqrt{\frac{\mathcal{U}_0}{t}}x,\, \sqrt{\frac{\mathcal{U}_1}{\mathcal{U}_0}}\right)\exp\left(\frac{ix^2}{8t}\right). \tag{51}$$

This solution exists provided $\mathcal{U}_0 > 0$ and $\mathrm{sgn}(\mathcal{U}_1) = \mathrm{sgn}(G_2)$. If the final component (k) of the Jacobi sn function is complex, the resulting sn function is still real-valued and hence we can have $\mathcal{U}_0$ and $\mathcal{U}_1 < 0$ simultaneously.

5. Analytic results for arbitrary spatial dimensions

Before continuing on to numerical simulations, we shall consider some analytical results for the cqGLE in spatial dimension greater than one, again assuming radial symmetry in the solutions. We consider the nonperturbative regime where either the potential or the amplitude of the solutions is large, obtaining various qualitative analytical results. When the kinetic energy term is small (relative to the nonlinearity and the confining potential), we recover the expected Thomas-Fermi approximation for the stationary solutions. We also outline the corresponding problem for wavefunctions with self-similar scalings.

5.1. Thomas-Fermi approximation

We consider a Thomas-Fermi approach, as summarised for the cubic-GPE case in [18]. We consider the repulsive case, so that both G_1 and G_2 are positive, and so look at the equation for $x \in \mathbb{R}^d$:

$$\nabla^2\psi(\boldsymbol{x}) = G_1|\psi(\boldsymbol{x})|^2\psi(\boldsymbol{x}) + G_2|\psi(\boldsymbol{x})|^4\psi(\boldsymbol{x}) + \Big(U(\boldsymbol{x}) - 1\Big)\psi(\boldsymbol{x}) \,. \tag{52}$$

Crucially for the Thomas-Fermi approximation, we suppose that there are a large number of BEC atoms, so that the condensate is very spread out due to the interatomic repulsion, and the density varies slowly in space. In this case, we may scale the space-variables to account for a slow variation of ψ in space, by defining $\hat{\boldsymbol{x}} = \sqrt{\epsilon}\boldsymbol{x}$ for a small real parameter $\epsilon << 1$. Writing $\phi(\hat{\boldsymbol{x}}) = \psi(\boldsymbol{x})$, we see that by chain rule $\nabla^2\psi(\boldsymbol{x}) = \epsilon\hat{\nabla}^2\phi(\hat{\boldsymbol{x}})$, where $\hat{\nabla}$ represents differentiation with respect to the $\hat{\boldsymbol{x}}$ variables. The stationary cqGPE (52) then becomes

$$\epsilon\hat{\nabla}^2\phi(\hat{\boldsymbol{x}}) = G_1|\phi(\hat{\boldsymbol{x}})|^2\phi(\hat{\boldsymbol{x}}) + G_2|\phi(\hat{\boldsymbol{x}})|^4\phi(\hat{\boldsymbol{x}}) + \Big(\hat{U}(\hat{\boldsymbol{x}}) - 1\Big)\phi(\hat{\boldsymbol{x}}) \,,$$

where we also write $\hat{U}(\hat{\boldsymbol{x}}) = U(\boldsymbol{x})$. Expanding the solution as $\phi(\hat{\boldsymbol{x}}) = \phi_0(\hat{\boldsymbol{x}}) + \epsilon\phi_1(\hat{\boldsymbol{x}}) + \cdots$, we see that to leading order, ϕ_0 solves

$$G_1|\phi_0(\hat{\boldsymbol{x}})|^2\phi_0(\hat{\boldsymbol{x}}) + G_2|\phi_0(\hat{\boldsymbol{x}})|^4\phi_0(\hat{\boldsymbol{x}}) + \Big(\hat{U}(\hat{\boldsymbol{x}}) - 1\Big)\phi_0(\hat{\boldsymbol{x}}) = 0 \,.$$

Since we are looking for non-trivial solutions, we may divide through by ϕ_0, obtaining the quadratic equation

$$G_2|\phi_0(\hat{\boldsymbol{x}})|^4 + G_1|\phi_0(\hat{\boldsymbol{x}})|^2 + \hat{U}(\hat{\boldsymbol{x}}) - 1 = 0 \,,$$

which has solutions

$$|\phi_0(\hat{\boldsymbol{x}})|^2_\pm = \frac{-G_1 \pm \sqrt{G_1^2 - 4G_2(\hat{U}(\hat{\boldsymbol{x}}) - 1)}}{2G_2} \,. \tag{53}$$

Since $G_1, G_2 > 0$, for $|\phi_0|^2$ to be real and positive we must take the "plus" root $|\phi_0|_+$, and require also that $\hat{U}(\hat{\boldsymbol{x}}) < 1$. In practice this requirement holds for many of the physically relevant potentials studied in this paper. It is satisfied for all confining potentials (in which $\hat{U}(\hat{\boldsymbol{x}}) < 0$), as well as positive potential functions such as the quantum pendulum and Morse potentials so long as these are sufficiently small. Putting the result back into physical coordinates,

$$|\Psi(\boldsymbol{x})|^2 = \frac{\sqrt{G_1^2 - 4G_2(U(\boldsymbol{x}) - 1)} - G_1}{2G_2} \,. \tag{54}$$

Compare this with the cGPE result, which is

$$|\Psi(\boldsymbol{x})|^2 = \frac{1 - U(\boldsymbol{x})}{G_1} \,, \tag{55}$$

and the qGPE result, given by

$$|\Psi(\boldsymbol{x})|^2 = \sqrt{\frac{1 - U(\boldsymbol{x})}{G_2}} \,. \tag{56}$$

5.2. Large potential limit

Another situation in which we may make progress analytically is when the potential is large, so $U(\boldsymbol{x}) = \epsilon^{-1}W(\boldsymbol{x})$ for small parameter $\epsilon << 1$. We anticipate that this will have an effect on the size of the solution ψ of the cqGPE

$$\nabla^2\psi(\boldsymbol{x}) = G_1|\psi(\boldsymbol{x})|^2\psi(\boldsymbol{x}) + G_2|\psi(\boldsymbol{x})|^4\psi(\boldsymbol{x}) + \Big(\epsilon^{-1}W(\boldsymbol{x}) - \mathrm{sgn}(G_1)\Big)\psi(\boldsymbol{x})\,, \tag{57}$$

and so scale $\psi(\boldsymbol{x}) = \delta^{-1}\varphi(\boldsymbol{x})$ for some small parameter $\delta(\epsilon) << 1$. Since the space variable $\boldsymbol{x}$ is unchanged we repress the arguments in the following discussion. With the scaling, (57) becomes

$$\delta^4\Big(\nabla^2\varphi + \mathrm{sgn}(G_1)\varphi\Big) = \delta^2 G_1|\varphi|^2\varphi + G_2|\varphi|^4\varphi + \frac{\delta^4}{\epsilon}W\varphi\,. \tag{58}$$

We look for a dominant balance between terms. If we attempt to form a dominant balance between the left-hand side with any term on the right we either obtain $\delta^4 \sim \delta^4\epsilon^{-1}$, or $\delta \sim 1$, both of which lead to the contradictory statement $1 >> \epsilon^{-1}$. Similarly, balancing the first two terms of the right hand side gives the contradictory $\delta = 1 >> \epsilon^{-1}$ again, and if we attempt to balance the first and third terms of the right hand side we obtain $\delta^2 \sim \epsilon$ and so the balance does not dominate the $O(1)$ term.

The only valid option therefore, is to form a balance between the second and third terms of the right-hand side of (58), so that $\delta = \epsilon^{1/4} << 1$. So in the limit as ϵ approaches zero, we have $W\varphi + G_2|\varphi|^4\varphi = 0$, and if φ is non-trivial, $|\varphi|^2 = \sqrt{\frac{-W}{G_2}}$, which in turn gives

$$|\Psi(\boldsymbol{x})|^2 = \sqrt{-\frac{U(\boldsymbol{x})}{G_2}} \tag{59}$$

for large U. Clearly this is only valid if the potential W and quintic coefficient G_2 have opposite signs. If $G_2 > 0$ then we require $U < 0$ (with $|U| >> 1$), corresponding to an attractive potential term. This makes physical sense since then a strong attractive potential, such as the harmonic potential $U(x) = -\epsilon^{-1}x^2$ for instance, which has the effect of concentrating mass at the origin, has a large magnitude density $\psi \sim \epsilon^{-1/4}$. Notice that if we take $U = \epsilon^{-1}W$ in the Thomas-Fermi solution (53) then to leading order in $\epsilon << 1$ we recover (59), and so this solution is the Thomas-Fermi solution in the case of a large amplitude potential.

5.3. Self-similar solutions in higher spatial dimensions

As we did in the 1D case, may consider a quasi-stationary solution which obeys a similarity scaling for the qGPE in $d > 1$ spatial dimensions. We consider solutions of (38) of the form $\Psi(\mathbf{x}, t) = t^{-1/2}\Phi(\eta)$, where $\eta = rt^{-1/2}$, while we also consider $V = V(\mathbf{x}, t) = t^{-1}\mathcal{U}(\eta)$. Substituting this into (38) we obtain

$$\Phi'' + \left(\frac{d-1}{\eta} - \frac{i\eta}{2}\right)\Phi' - \frac{i}{4}\Phi = G_2|\Phi|^4\Phi - \mathcal{U}(\eta)\Phi\,, \tag{60}$$

where prime denotes differentiation with respect to the similarity variable η. Writing $\Phi(\eta) = R(\eta)e^{i\theta(\eta)}$, we obtain the real system

$$R'' + \frac{d-1}{\eta}R' - R\theta'^2 + \frac{\eta}{2}R\theta' - \mathcal{U}(\eta)R - G_2R^5 = 0\,, \tag{61}$$

$$R\theta'' + 2R'\theta' + \frac{d-1}{\eta}R\theta' - \frac{1}{4}R - \frac{\eta}{2}R' = 0\,. \tag{62}$$

We can integrate (62) for θ', and then integrating again we find

$$\theta(\eta) = \theta(0) + \theta'(0)\int_0^\eta \frac{dy}{y^{d-1}(R(y))^2} + \frac{1}{4}\int_0^\eta \frac{\int_0^y (R(z) + 2zR'(z))\,R(z)z^{d-1}dz}{y^{d-1}(R(y))^2}dy\,. \tag{63}$$

However, substituting this into (61) would give a complicated nonlinear integral equation. Indeed, the appearance of the $(d-1)/\eta$ factor means that exact solutions are even harder to come by. However, numerical simulations are possible. We plot solutions for fixed $\mathcal{U}(\eta) = 0$ for various dimension of space $d = 1, 2, 3$ in Figure 2. We see that, as the dimension of the space increases, the oscillations away from the origin are damped, although the remainder of the structure is similar between spatial dimensions.

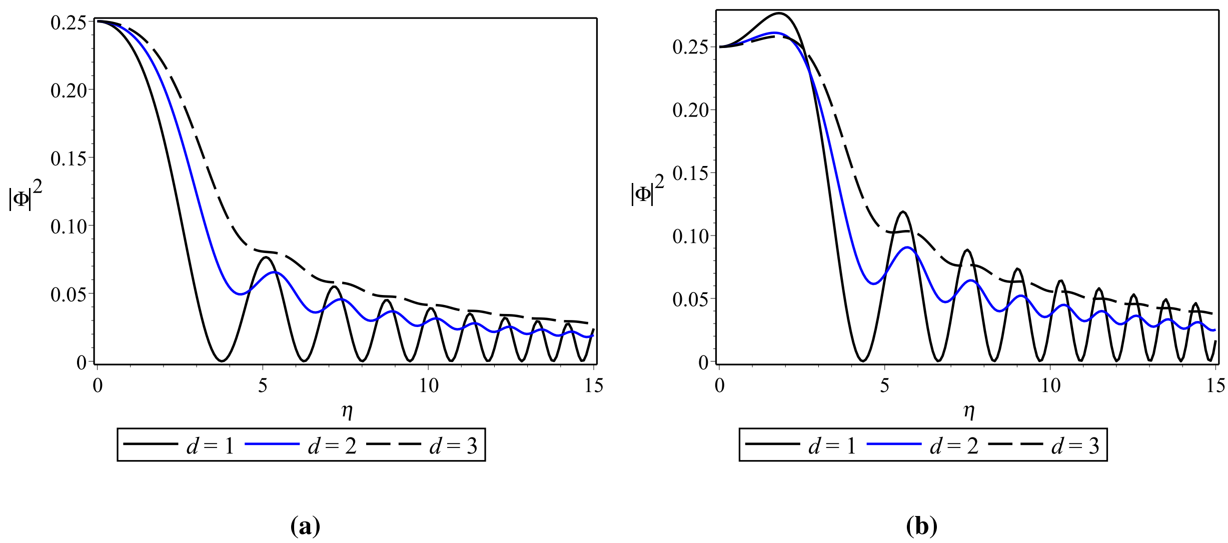

Figure 2: Self-similar solutions in one, two, or three spatial dimensions obtained by solving (61)-(62) for $\mathcal{U}(\eta) = 0$ and (a) $G_2 = -1$, (b) $G_2 = 1$. We take conditions $R(0) = 0.5$, $R'(0) = 0$, $\theta'(0) = 1$.

6. Numerical simulations for various confining potentials and resulting dynamics

For more complicated potentials, unbounded potentials, or potentials which grow to size $O(\epsilon^{-1})$, the aforementioned analytical results will lose validity. As such, will shall now find numerical solutions for the cqGPE when a confining potential $U(x)$ is applied (viewing these solutions as small or large perturbations about the zero-potential solutions, when relevant). We will look at the effects of a variety of specific potentials which are of physical relevance, the same as those used in [12, 13, 14, 15], in order to provide comparison between the cubic and cubic-quintic models. All numerical simulations in this paper are performed in MATLAB, using the differential equation solver "ode45". We organise the solutions by first looking at the case when the two-particle interaction is attractive, so that the cubic coefficient $G_1 < 0$, and then the case where these interactions are repulsive and $G_1 > 0$. Within each section we then consider different forms of potential functions $U(x)$, and different values of G_2. By fixing the constant a we may choose $|G_1| = 1$ without loss of generality, which we will often do.

To illustrate our results, we shall consider six unique confining potentials.

- The *harmonic potential* is given by $U(x) = \lambda x^2$, where λ is real-valued. This potential models a parabolic BEC trap, which confines the BEC to a central area about $x = 0$. It has been used frequently for both cubic and quintic-cubic models in the literature, for instance in [44, 45, 46, 47]. In $d = 2, 3$, the harmonic potential reads $U(r) = \lambda r^2$.

- The harmonic potential in the previous section is often modified in a variety of ways, as for instance in [48, 49]. We will use an *exponentially modified harmonic potential*, $U(x) = \lambda(x^2 + \beta e^{-x^2})$, with λ, β constants. In $d = 2, 3$, the exponentially modified harmonic potential reads $U(r) = \lambda(r^2 + \beta e^{-r^2})$.

- The *Morse potential* is the asymmetric function $U(x) = \lambda(e^{-2Ax} - 2e^{-Ax})$, used for instance in [50, 51]. We take $\lambda < 0$ so that solutions remain bounded, and the potential forces the mass on one side of the origin to decay to zero, leaving it largely unchanged on the other, like a crude "step"-function. We also only take $A > 0$, although the $A < 0$ case is merely the reflection of the $A > 0$ plot about $x = 0$. In $d = 2, 3$, the radial Morse potential reads $U(r) = \lambda(e^{-2Ar} - 2e^{-Ar})$.

- The *quantum pendulum potential* is given by $U(x) = \lambda(1 - \cos(x))$ where λ is a constant. It models an optical lattice trap well, with the multiple peaks and troughs of the cosine function characterising the lattice of traps.

Similar trigonometric traps are considered in [52, 53, 54]. In $d = 2, 3$, the radial quantum pendulum potential reads $U(r) = \lambda(1 - \cos(r))$.

- The *double-well potential* models a trap with two wells, symmetric about $x = 0$, and is given by $U(x) = \epsilon\lambda[(x^2 - 1)^2 - \beta]$. Such models have been used in various studies, such as [55, 56, 57]. In $d = 2, 3$, the radial double-well potential reads $U(r) = \lambda[(r^2 - 1)^2 - \beta]$.

- The harmonic potential may be combined with a lattice potential, for instance by taking $U(x) = \lambda(x^2 + \beta\cos^2(x))$, as we do here, resulting in a quasi-periodic potential referred to as the *harmonic potential with lattice trap*. This type of potential has been often used, for example in [58, 59]. In $d = 2, 3$, the radial harmonic potential with a lattice trap reads $U(r) = \lambda(r^2 + \beta\cos^2(r))$.

With the confining potentials of interest defined, we now turn to numerical simulations. In Figures 3-5 we plot stationary BECs in the attractive case ($G_1 < 0$) in 1D, 2D, and 3D, respectively. With regard to the dimension of the space, we find than an increase in d results in a dampening of the small oscillations seen removed from the origin, although the overall qualitative dynamics appear similar. The Morse potential solution become confined to near the origin for $d = 3$, while for $d = 1, 2$ the solutions oscillate about a positive, constant level of density in space. Hence, increasing the spatial dimension may mitigate the effects from confining potentials, requiring a modification of the potential if one wishes to preserve the behavior seen for $d = 1$.

In Figures 6-8 we plot stationary BECs in the repulsive case ($G_1 > 0$) in 1D, 2D, and 3D, respectively. Compared to the attractive case, the repulsive solutions exhibit even greater regularization as the dimension of the space increases, with more of the BEC confined to near the origin as d increases. For $d = 3$, the differences between results for various confining potentials become more pronounced than they do, say, in the $d = 1$ case.

As anticipated, once the increased damping with spatial dimension is accounted for, most of the differences in the various numerical simulations are due to the particular confining potential selected. We find that for the double-well, Morse, and harmonic potentials and for variants on the harmonic potential, we require $\lambda < 0$ for physically relevant solutions. Physically, this corresponds to the potentials restricting the BEC particles to certain regions of space. The quantum pendulum potential is an exception, with $\lambda > 0$ solutions bounded for most values of G_1 and G_2. However, for $G_1 > 0$ and large enough $G_2 > 0$ the solutions under the quantum pendulum potential became unbounded for all λ, even $\lambda < 0$. In general results are similar to those obtained in [12, 13] in the case of the cGPE. The effect of the quintic term in the equation may be seen, however, in the plots in which the potential parameters are fixed. Here we generally see an increase in G_2 causing greater amplitude local maxima away from the origin, and in some cases, such as the double-well potential, changes in G_2 greatly affect the shape of the density $|\psi|^2$ near the origin. We would expect that the effect of the quintic term would be most obvious in regions where the density $|\psi|^2$ is not too small, since if this becomes too small then the quintic term will clearly be dominated by the cubic and linear terms. In practice, this means that we see greater effects of the quintic term near the origin.

Regarding the 2D solutions to (11) under various small external potentials $U(r)$, and with various values of G_1 and G_2, we found that unlike in 1D, the zero-potential solutions, while still oscillatory, no longer have fixed amplitude, but decay as r increases, either to a constant if $G_1 < 0$, or to zero if $G_1 > 0$. In either case for large enough positive G_2 the solutions instead diverge. Since the zero-potential equation is mathematically equivalent to the constant-potential equation (if this constant is small enough), we know that solutions under a constant potential are scaled versions of those already discussed.

If $U(r)$ is the double-well potential, harmonic potential, or modification of the harmonic potential, the quadratic term in the potential causes solutions to become unbounded for $\lambda > 0$, as in 1D. The physically relevant solutions are those with $\lambda < 0$, and so the BEC is confined to some localized region of space. The Morse potential may no longer be viewed as a "step"-potential (forcing the mass to one side of the origin) as we viewed it in 1D, since now we take only $r > 0$. Indeed, we may now obtain physically relevant solutions for $\lambda > 0$ so long as $A > 0$. A particularly interesting result for the Morse potential is that we see an unbounded solution for $\lambda < 0$, so long as we take $A > 0$ and ϵ large enough. We also see unexpected behaviour under the quantum pendulum potential. For $G_1 < 0$, the solutions under the quantum pendulum potential behave fairly regularly, although they do not decay in amplitude despite the oscillations of the underlying zero-potential solutions decaying to a constant. For $G_1 > 0$ the situation is very different, with $\lambda < 0$ solutions decaying along with the unperturbed zero-potential solution if $G_2 > 0$, but diverging for $\lambda > 0$.

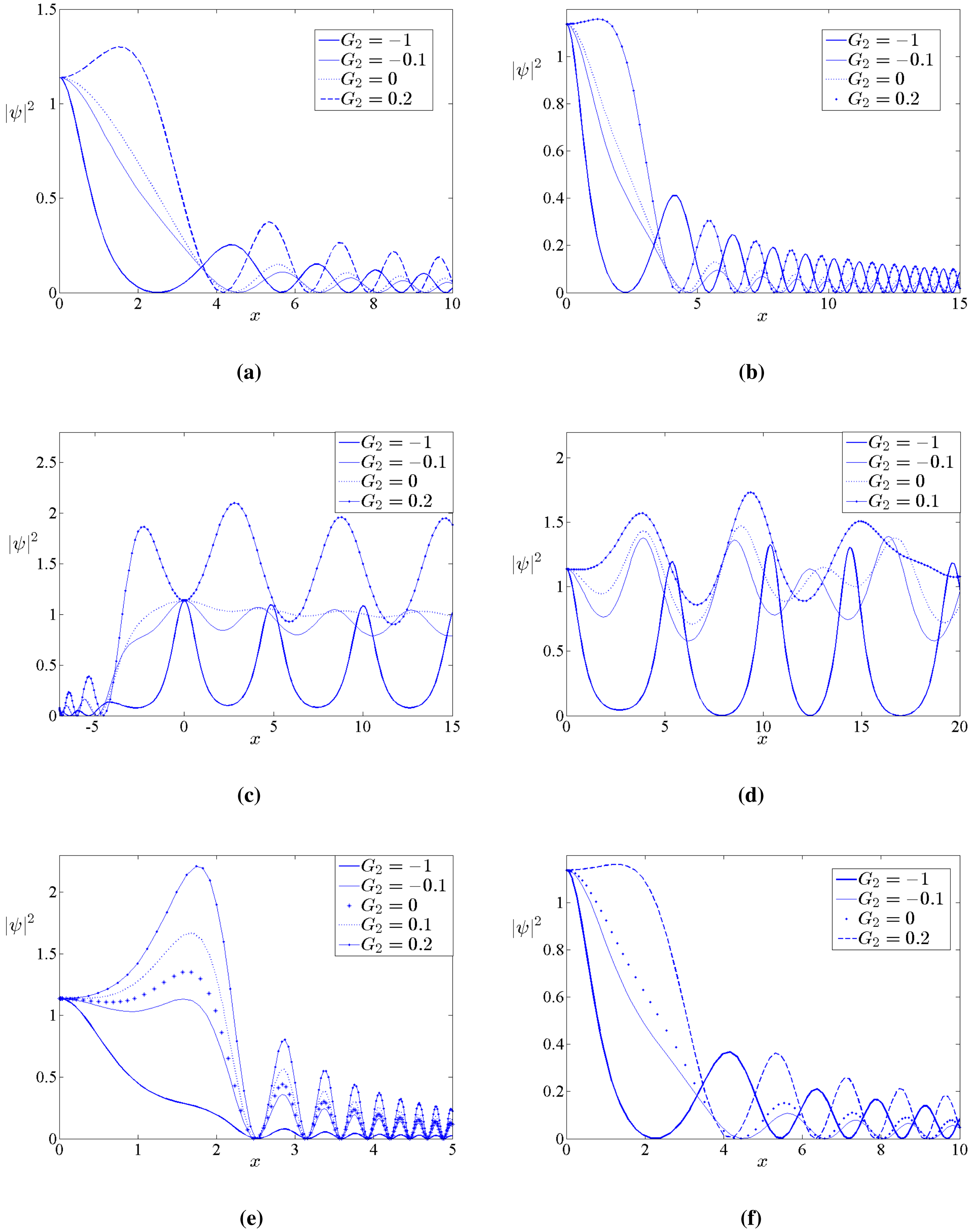

Figure 3: Stationary solutions to the attractive GPE under various potentials in 1D geometry for various strengths of the quartic nonlinearity term G_2. The potentials considered are (a) harmonic potential ($\lambda = -0.1$), (b) exponentially modified harmonic potential ($\lambda = -0.1, \beta = 1$), (c) Morse potential ($\lambda = -0.1, A = 0.4$), (d) quantum pendulum potential ($\lambda = -0.1$), (e) double-well potential ($\lambda = -0.5, \beta = 1$), (f) harmonic potential with lattice trap ($\lambda = -0.1, \beta = 1$). We set $G_1 = -1$ for all plots.

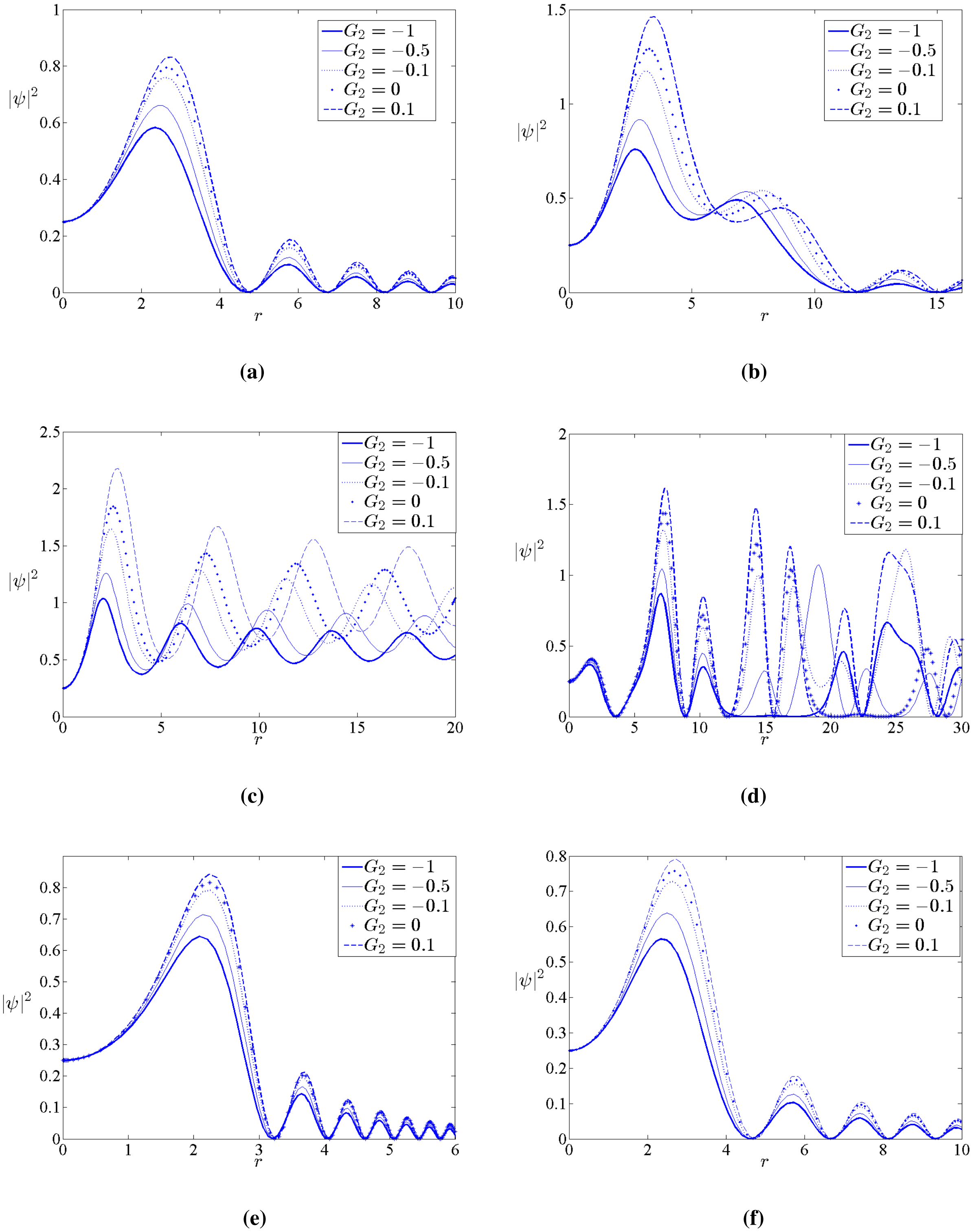

Figure 4: Stationary solutions to the attractive GPE under various potentials in 2D radially symmetric geometry for various strengths of the quartic nonlinearity term G_2. The potentials considered are (a) harmonic potential ($\lambda = -0.1$), (b) exponentially modified harmonic potential ($\lambda = -0.01$, $\beta = 1$), (c) Morse potential ($\lambda = -1$, $A = 0.4$), (d) quantum pendulum potential ($\lambda = -1$), (e) double-well potential ($\lambda = -0.5, \beta = 1$), (f) harmonic potential with lattice trap ($\lambda = -0.1, \beta = 1$). We set $G_1 = -1$ for all plots.

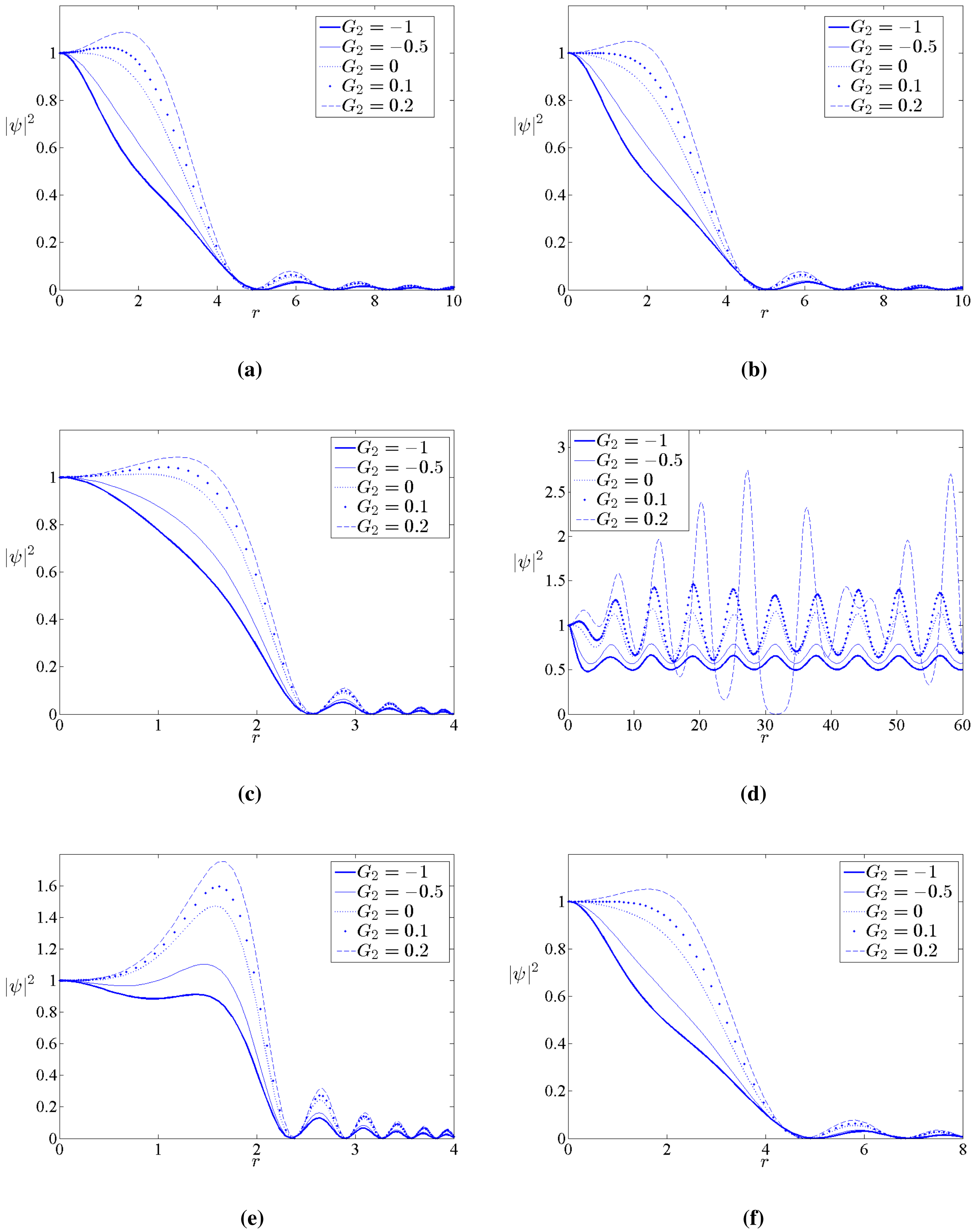

Figure 5: Stationary solutions to the attractive GPE under various potentials in 3D radially symmetric geometry for various strengths of the quartic nonlinearity term G_2. The potentials considered are (a) harmonic potential ($\lambda = -0.1$), (b) exponentially modified harmonic potential ($\lambda = -0.01$, $\beta = 1$), (c) Morse potential ($\lambda = -0.1$, $A = 0.4$), (d) quantum pendulum potential ($\lambda = -0.1$), (e) double-well potential ($\lambda = -1$, $\beta = 1$), (f) harmonic potential with lattice trap ($\lambda = -0.1, \beta = 1$). We set $G_1 = -1$ for all plots.

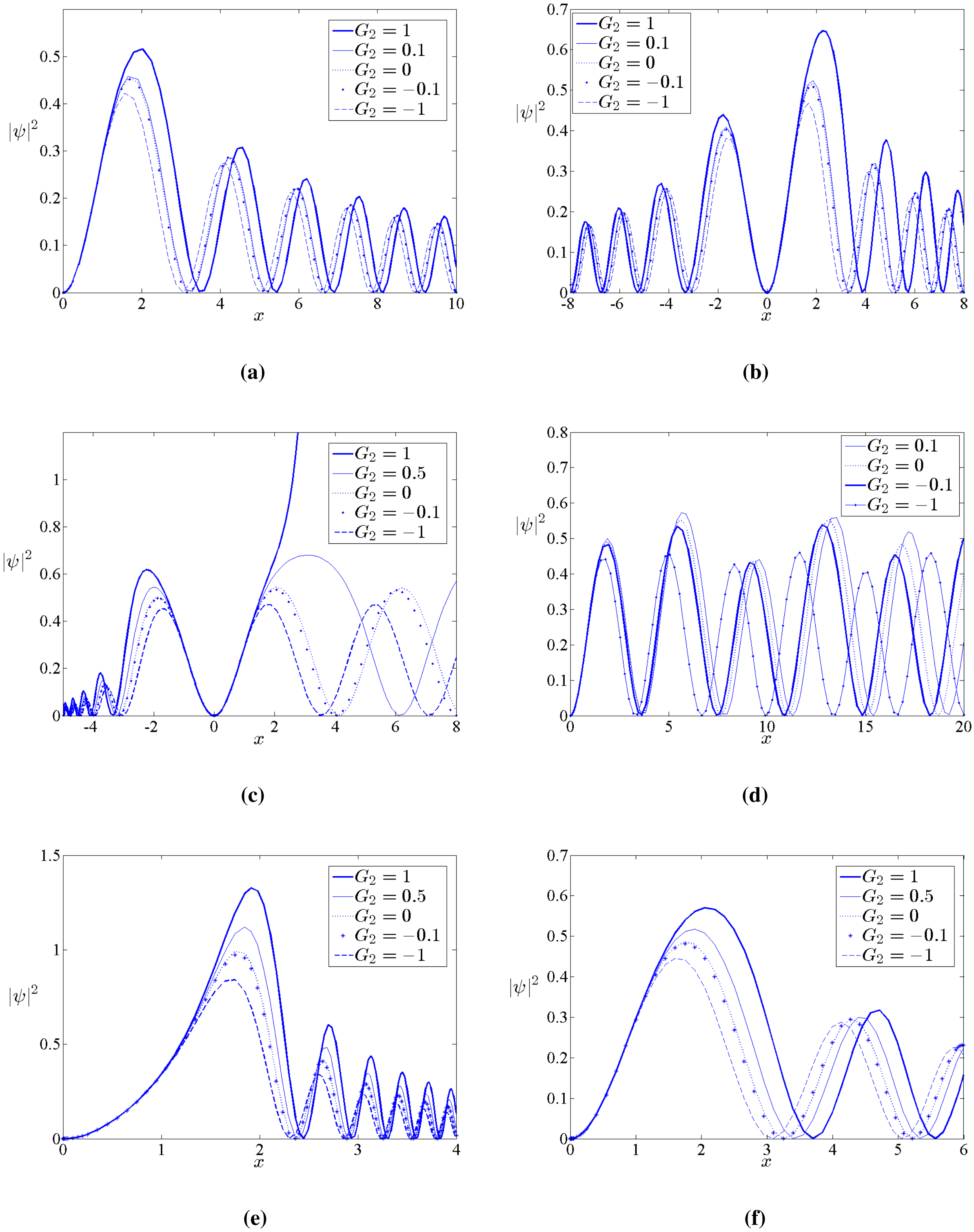

Figure 6: Stationary solutions to the repulsive GPE under various potentials in 1D geometry for various strengths of the quartic nonlinearity term G_2. The potentials considered are (a) harmonic potential ($\lambda = -0.1$), (b) exponentially modified harmonic potential ($\lambda = -0.1, \beta = 0.5$), (c) Morse potential ($\lambda = -0.01, A = 1$), (d) quantum pendulum potential ($\lambda = -0.1$), (e) double-well potential ($\lambda = -1, \beta = 1$), (f) harmonic potential with lattice trap ($\lambda = -0.1, \beta = -1$). We set $G_1 = 1$ for all plots.

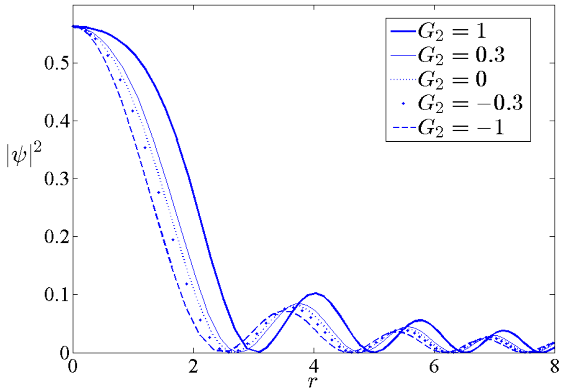

(a)

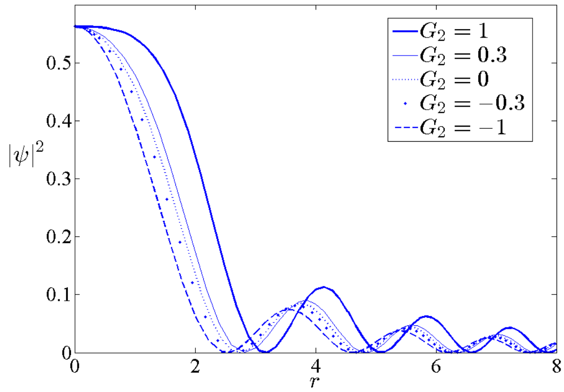

(b)

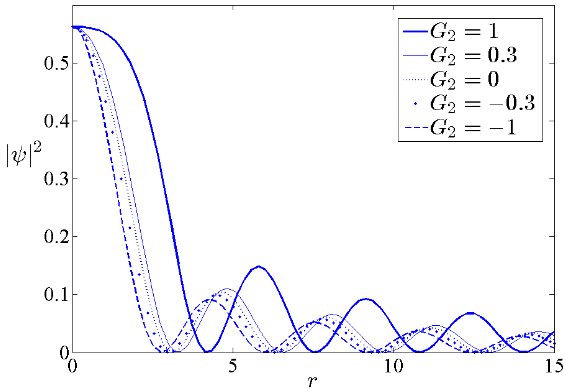

(c)

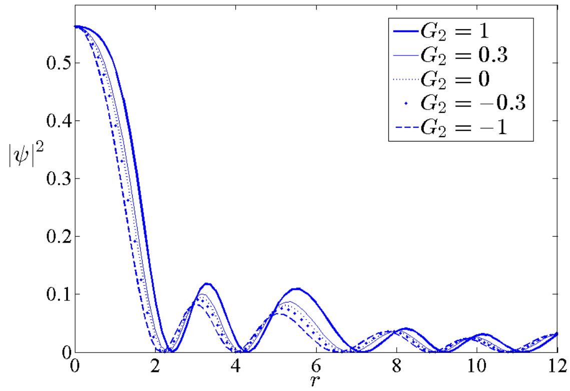

(d)

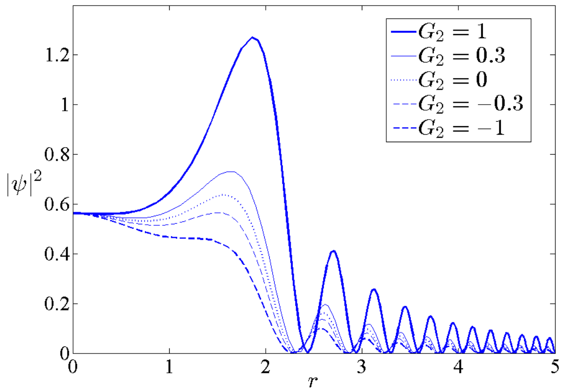

(e)

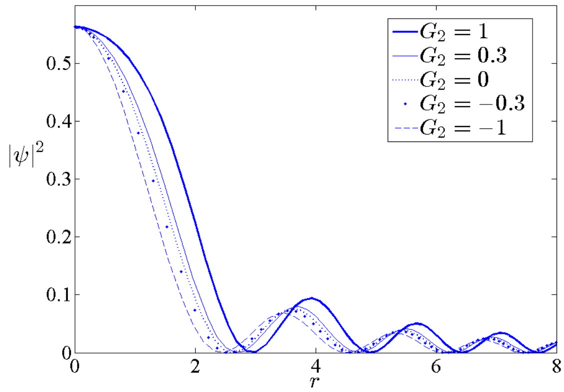

(f)

Figure 7: Stationary solutions to the repulsive GPE under various potentials in 2D radially symmetric geometry for various strengths of the quartic nonlinearity term G_2. The potentials considered are (a) harmonic potential ($\lambda = -0.1$), (b) exponentially modified harmonic potential ($\lambda = -0.1$, $\beta = -1$), (c) Morse potential ($\lambda = -0.1$, $A = 1$), (d) quantum pendulum potential ($\lambda = -1$), (e) double-well potential ($\lambda = -1, \beta = 1$), (f) harmonic potential with lattice trap ($\lambda = -0.1, \beta = 1$). We set $G_1 = 1$ for all plots.

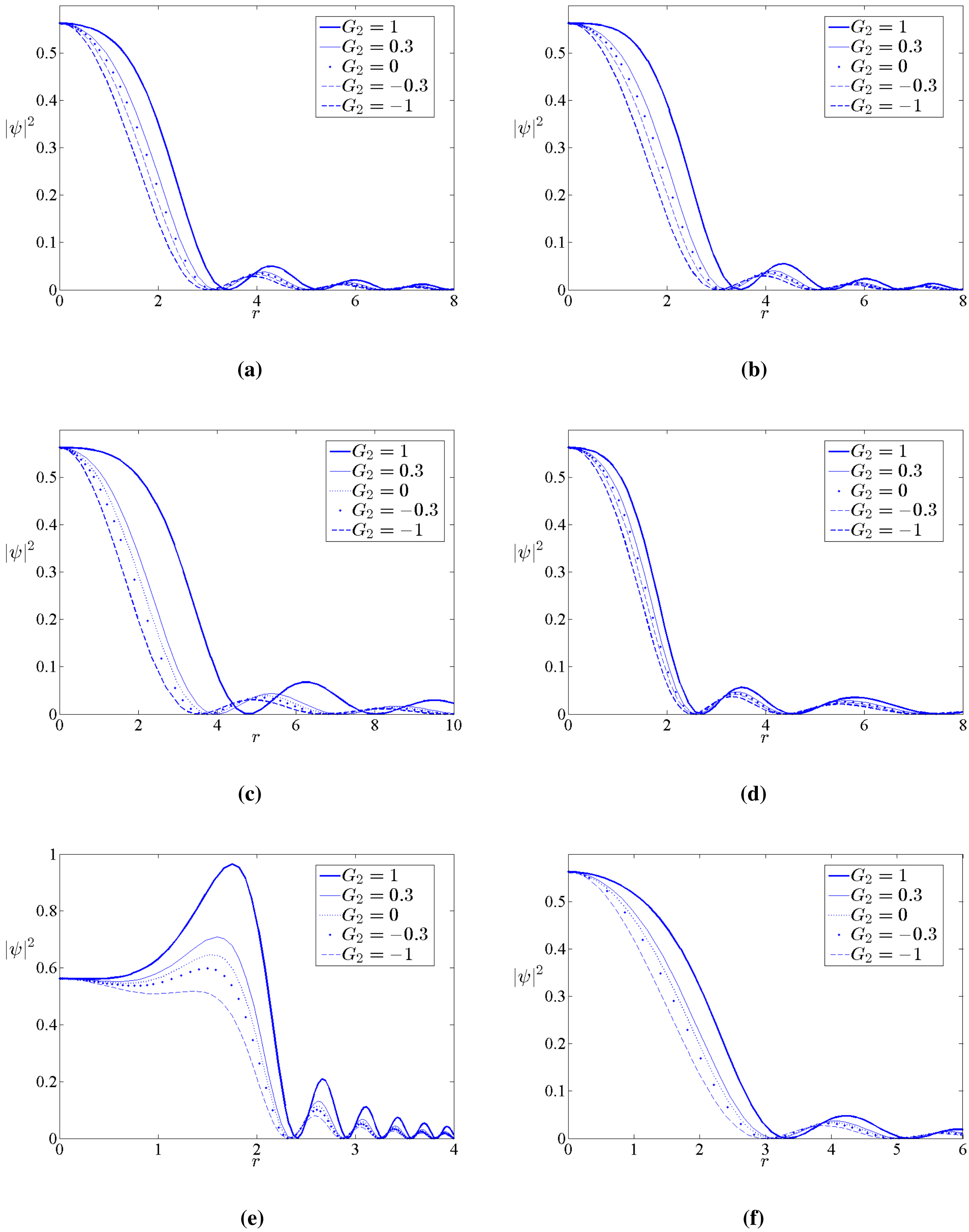

Figure 8: Stationary solutions to the repulsive GPE under various potentials in 3D radially symmetric geometry for various strengths of the quartic nonlinearity term G_2. The potentials considered are (a) harmonic potential ($\lambda = -0.1$), (b) exponentially modified harmonic potential ($\lambda = -0.1$, $\beta = -1$), (c) Morse potential ($\lambda = -0.1$, $A = 1$), (d) quantum pendulum potential ($\lambda = -1$), (e) double-well potential ($\lambda = -1, \beta = 1$), (f) harmonic potential with lattice trap ($\lambda = -0.1, \beta = 1$). We set $G_1 = 1$ for all plots.

In the $G_1 > 0, G_2 < 0$ case, the $\lambda > 0$ solutions decay for small enough ϵ along with the $\lambda < 0$ solutions, but we see an instability if ϵ is large enough.

Many of these results are in agreement with those of [14], but the different effects seen here for different values of G_2 under the quantum pendulum and Morse potentials especially, highlight some subtle differences between the cubic and cubic-quintic GPE models.

The 3D radial solutions found are often very similar to those found in the 2D case, which is unsurprising considering the similarity between the radially symmetric equations (8) and (10). In general, we see decaying solutions decay faster in the 3D case than in the 2D case, which, as mentioned above, results in more of the BEC being confined to near the origin. Aside from the slightly faster rate of decay, solutions under the quadratic-based potentials (such as those based around the harmonic potential, and the double-well potential) retain similar characteristics in 3D to those in lower dimensions, becoming unbounded for $\lambda > 0$ and forcing the density $|\psi|^2$ to decay in the relevant regions for $\lambda < 0$.

We see more interesting results for the Morse potential in 2D and 3D, with $\lambda > 0$ giving bounded results for positive A, for G_1 and G_2 positive or negative. We also see an instability appear in the case of $\lambda < 0$ for large enough A and ϵ. This only seems to occur in the $G_1, G_2 > 0$ case, and perhaps is merely indicative of an instability in the underlying zero-potential solution for large enough positive G_2.

The quantum pendulum potential also gives some unexpected results, with all solutions becoming unstable and diverging in finite time when $G_1 < 0$ and $G_2 > 0$, and becoming unstable but remaining oscillatory when $G_1 > 0$ and $G_2 < 0$ if ϵ is sufficiently large.

6.1. Asymptotic dynamics near spatially uniform states

It was pointed out in [25] that solutions for the cGPE without confining potential (so, the cubic NLS equation) exhibit a change in wavelength in space under certain conditions. In particular, when the solution is close to one spatially uniform state it will exhibit one wavelength, while near another spatially uniform state it will exhibit a different wavelength. Such behaviors can also be found in the cqGLE in Figure 4b, for instance, we see such behavior. Additionally, near a spatially uniform state, a solution may oscillate (or exhibit damped oscillation) in space. This behavior is see in Figures 3c, 3d, 4c, and 4d.

In order to better understand the structure of solutions in such regimes, we shall consider asymptotics of solutions near spatially uniform states. To make the analysis more tractable we shall set the spatial potential to zero, although, as seen in the aforementioned figures, such behaviors are still observed in the case where confining potentials are non-zero. For $U(r) = 0$, we have

$$\psi'' + \frac{d-1}{r}\psi' = G_1\psi^3 + G_2\psi^5 - \mathrm{sgn}(G_1)\psi\,. \tag{64}$$

Consider a perturbation of the form

$$\psi(r) = \overline{\psi} + \epsilon\hat{\psi}(r)\,, \tag{65}$$

where $\overline{\psi}$ denotes a spatially uniform state which is a solution to

$$G_1\overline{\psi}^3 + G_2\overline{\psi}^5 - \mathrm{sgn}(G_1)\overline{\psi} = 0\,, \tag{66}$$

$0 < \epsilon << 1$ is a small parameter, and $\hat{\psi}(r)$ is a perturbation giving the local behavior of a solution near $\overline{\psi}$. Note that there are at most five real solutions from (66) (by assumption, we rule out complex solutions, of which there are exactly five). We have that $\overline{\psi} = 0$ is always a solution, while other solutions are determined by

$$\overline{\psi}^2 = \frac{-G_1 \pm \sqrt{G_1^2 + 4G_2\mathrm{sgn}(G_1)}}{2G_2} \tag{67}$$

if $G_2 \neq 0$ or

$$\overline{\psi}^2 = \frac{1}{|G_1|} \tag{68}$$

if $G_2 = 0$ yet $G_1 \neq 0$. Solutions $\overline{\psi} \neq 0$ are obtained from parameter values G_1 and G_2 making the right hand side of (67)-(68) positive. Depending on the parameter values, there may be from zero to four non-zero values of $\overline{\psi}$.

Assume that we pick one such $\overline{\psi} \in \mathbb{R}$. Placing (65) into (64), then at $O(1)$ we recover (66) while at $O(\epsilon)$ we have that the perturbation $\hat{\psi}(r)$ satisfies

$$\hat{\psi}'' + \frac{d-1}{r}\hat{\psi}' = \left\{3G_1\overline{\psi}^2 + 5G_2\overline{\psi}^4 - \mathrm{sgn}(G_1)\right\}\hat{\psi}\,. \tag{69}$$

When $d = 1$ we have that

$$\hat{\psi}(r) = C\sin\left(\mu(\overline{\psi}, G_1, G_2)(r - r_0)\right) \tag{70}$$

where C and r_0 are real constants, while

$$\mu(\overline{\psi}, G_1, G_2) = \sqrt{\mathrm{sgn}(G_1) - 3G_1\overline{\psi}^2 - 5G_2\overline{\psi}^4}\,. \tag{71}$$

Such a solution only exists if $\mu(\overline{\psi}, G_1, G_2) > 0$, otherwise an asymptotic expansion of this form does not exist near the choice of $\overline{\psi}$. This failure could result from the spatially uniform state being strongly repulsive (unstable as a dynamical system) or not existing for the parameters G_1 and G_2 used.

When $d = 2$ we have that

$$\hat{\psi}(r) = CJ_0\left(\mu(\overline{\psi}, G_1, G_2)(r - r_0)\right) \sim (r - r_0)^{-1/2}\sin\left(\mu(\overline{\psi}, G_1, G_2)(r - r_0) - \frac{\pi}{4}\right) + O\left(r^{-1}\right), \tag{72}$$

while when $d = 3$ we have

$$\hat{\psi}(r) = C(r - r_0)^{-1}\sin\left(\mu(\overline{\psi}, G_1, G_2)(r - r_0)\right). \tag{73}$$

More generally, we find that for $d \geq 1$,

$$\hat{\psi}(r) \sim (r - r_0)^{(1-d)/2}P(r - r_0) \quad \text{as} \quad r \to \infty\,, \tag{74}$$

where P is a bounded periodic function with period $2\pi\mu(\overline{\psi}, G_1, G_2)$. This gives the local wavelength $L(\overline{\psi}) = 2\pi\mu(\overline{\psi}, G_1, G_2)$, and this changes in a neighborhood of each spatially uniform state.

While our results explain the structure of stationary states far from the origin, they also help us to understand why solutions may appear to change wavelength over intermediate length scales closer to the origin, as was also pointed out in [25] for related cubic NLS solutions. Indeed, when a solution initially may start near a spatially uniform state $\overline{\psi}_1$ resulting in local wavelength $L(\overline{\psi}_1)$, the solution may end up attracted to a stable spatially uniform state $\overline{\psi}_2$ resulting in a new local wavelength $L(\overline{\psi}_2)$.

6.2. *Purely quintic self-interactions*

As we have done for the cqGLE, we may also consider numerical solutions for stationary solutions in the qGPE in order to understand the role of the confining potential. As cubic, quintic, and potential terms are now no longer competing for dominance, we can rescale so that there is one scaling parameter in the problem, namely the ratio of the parameter scaling the potential and the parameter G_2. Then, (40) is put into the form

$$\hat{\psi}'' = \mathrm{sgn}(G_2)(\hat{\psi}^5 - \hat{\psi}) + \hat{U}(x)\hat{\psi}\,, \tag{75}$$

where the functions have absorbed a factor of $|G_2|^{-1/4}$, i.e. $\psi(x) = |G_2|^{-1/4}\hat{\psi}(x)$ and $U(x) = |G_2|^{-1/4}\hat{U}(x)$. When $\hat{U}(x) = 0$, the solutions remain bounded for $G_2 < 0$ given any value of $\hat{\psi}(0)$. For $G_2 > 0$, the solutions remain bounded only for $|\hat{\psi}(0)| < 1$.

Solving (75) numerically for various potentials, we find qualitatively similar results. The $G_2 > 0$ case tends to be more stable, as alluded to above for the base solution with zero potential. However, the solutions can become unbounded for large enough positive λ. When $G_2 < 0$, then strong enough $\lambda < 0$ can be stabilizing. As the results are qualitatively similar to earlier solutions, we do not provide detailed plots here for the qGPE.

7. Discussion

We have studied stationary and quasi-stationary solutions for the cubic-quintic Gross-Pitaevskii equation modeling Bose-Einstein condensates (BECs) in one, two, and three spatial dimensions under the assumption of radial symmetry. Further, we considered dynamics influenced by a variety of different confining potentials. We considered both repulsive and attractive cubic interactions for the cubic nonlinear term (modeling repulsive and attractive two-body interactions) as well as quintic nonlinearity (modeling the strength of inter-atomic coupling). Analytical solutions, including some new exact solutions for the 1D case, were obtained for constant (including zero) or small confining potentials. Numerical solutions were obtained for cases where the confining potential is more dominant.

In Section 3 we obtained a number of exact solutions to the 1D case, generalizing bright and dark soliton solutions of the cubic NLS or GP equations. We also obtain exact periodic solutions in these cases, generalizing the cnoidal, snoidal, and dnoidal solutions for the cubic NLS equation. To deal with the case where the potential is non-constant, we also carried out a perturbation analysis in 1D in the case of a general, small, space-dependent potential function in Section 3. Here we obtained explicit expressions for all higher order corrections to the leading order solution, allowing the asymptotic expansion of the solution to be found, in theory, up to any degree of accuracy. In practice, the perturbation solutions were observed to match numerical solutions well near the origin, even just taking the first order correction. However, for many of the potentials studied in the literature, the potential grows as x increases. This, along with the fact that the leading order density $|\psi_0|^2$ often decays as we move away from the origin, and that the derivative $\psi_0'(x)$ must approach zero, means that the small potential assumption is often invalidated for large enough x. For such cases, this motivates the need for numerical simulations. We have seen soliton and periodic solutions of the zero-potential equations (13) and (17), and shown that the situation of $U(x)$ = constant is mathematically equivalent to the situation $U(x) = 0$ (so long as the constant is sufficiently small). We have solved (6) for a variety of specific small external potentials $U(x)$. The exact dark solitary wave for the cqGPE, as well as the exact spatially periodic solutions, appear to be new, and generalize results for the cGPE in the literature.

In Section 4, we focused on the case where the nonlinearity is purely quintic. We again gave exact stationary solutions for specific potential functions. Bright or dark soliton solutions, as well as periodic solutions, can be found from the analogous results in Section 3 by taking the $G_1 \to 0$ limit, subject to relevant parameter restrictions being obeyed. We also considered self-similar solutions, again for specific external potentials, obtaining exact self-similar solutions corresponding to quasi-stationary wavefunctions.

While general perturbation solutions are not possible for spatial dimensions greater than one (due to lack of exact solutions to the unperturbed problem), there are still some asymptotic limits to be considered which result in analytically tractable cases, and these were studied in Section 5. In limits where the kinetic energy of small relative to the potential (the Thomas-Fermi approximation) or when the potential is very large, then the density of the BEC can be approximated (to first order) in terms of the confining potential. This requires a balance between the potential and self-interaction terms, and hence the precise form of the lowest order result will differ between the cGPE, qGPE, and cqGPE. We also mention the problem of self-similar wavefunctions in spatial dimensions greater than one.

The numerical solutions of Section 6 generally give good specific results, showing the effect of some particular space-dependent confining potentials on the solutions of the stationary equation. In each case, the potential is scaled with a factor λ. While many of the results in this paper are similar to those in the cubic case studied in [14, 15], we do see some effect of the sign of G_2 in the qualitative behavior of solutions under specific potentials (namely the quantum pendulum and Morse potentials, as described above). We also see the effect of the quintic term more subtly in the shape of solutions for the quadratic-based potentials, as shown in the plots with fixed potential parameters, and only G_2 varied. An increase in G_2 often results in a greater amplitude local maxima away from the origin, and in some cases, such as the double-well potential, changes in will G_2 affect the shape of the density $|\psi|^2$ near the origin.

We have also considered stationary solutions for the cqGPE in two and three spatial dimensions. The BEC solutions were confined using radial external potentials, which in turn induce radial wavefunction solutions. The assumption of radial symmetry gives 2D cylindrical (or, cigar-shaped) and 3D spherical BECs. We consider results for both attractive and repulsive two-body interactions, akin to what was done for purely cubic self-interactions in [14, 15], and we then deduce the role of corrections due to strong inter-atomic coupling for each regime. We found that unlike in 1D, the zero-potential solutions, while still oscillatory, no longer have fixed amplitude, but decay as r increases, either to a constant if $G_1 < 0$, or to zero if $G_1 > 0$. In some parameter regimes, the parameters of the confining potential are essential to the regularity of solutions, while for other parameter regimes there can be divergence of the wavefunction.

Hence, care is needed when selecting the parameter regime. Many of these results are again in agreement with those of [14], but the different effects seen here for different values of G_2 under the quantum pendulum and Morse potentials especially, highlight some subtle differences between the cubic and cubic-quintic GPE models.

Noticing that solutions tend to oscillate around uniform states sufficiently far from the origin, we have carried out an asymptotic analysis of solutions near spatially uniform states. These results help in determining wavelength and damping date sufficiently far from the origin. Such results are also useful in explaining why solutions appear to change wavelength over intermediate length scales closer to the origin. As the solution moves from between one spatially uniform state which is repulsive to another spatially uniform state which is attractive, the wavelength (calculated near each uniform state) will be modified. Such behavior was previously described for the cubic NLS equation in the attractive self-interaction case in [25].

Further work could attempt to extend the results found in this paper to the full spatial problem without assuming radial symmetry, or to include non-stationary solutions for the cqGPE. An example of non-stationary solutions which could still be studied using ODEs rather than a full PDE would be quasi-steady solutions which exhibit a form of self-similarity. Another possibility would be to consider relativistic BECs under the relevant nonlinear Klein-Gordon model with a quintic nonlinearity term. This was recently done for strictly cubic nonlinear interactions [60], with the results of some relevance, e.g. to neutron stars. One could also attempt to study the stability (such as spectral or orbital stability [16, 61, 62, 63, 64]) of particular analytical or exact solutions under small potentials.

[1] E. Cornell, C. Wieman, Nobel Lecture: Bose-Einstein condensation in a dilute gas, the first 70 years and some recent experiments, Reviews of Modern Physics 74 (3) (2002) 875.

[2] W. Ketterle, Nobel Lecture: When atoms behave as waves: Bose-Einstein condensation and the atom laser, Reviews of Modern Physics 74 (4) (2002) 1131.

[3] M. Matthews, B. Anderson, P. Haljan, D. Hall, C. Wieman, E. Cornell, Vortices in a Bose-Einstein condensate, Physical Review Letters 83 (13) (1999) 2498.

[4] J. Williams, M. Holland, Preparing topological states of a Bose-Einstein condensate, Nature 401 (6753) (1999) 568–572.

[5] Y. Ovchinnikov, J. Müller, M. Doery, E. Vredenbregt, K. Helmerson, S. Rolston, W. Phillips, Diffraction of a released Bose-Einstein condensate by a pulsed standing light wave, Physical Review Letters 83 (2) (1999) 284.

[6] D. Jaksch, C. Bruder, J. Cirac, C. W. Gardiner, P. Zoller, Cold bosonic atoms in optical lattices, Physical Review Letters 81 (15) (1998) 3108.

[7] B. Anderson, M. Kasevich, Macroscopic quantum interference from atomic tunnel arrays, Science 282 (5394) (1998) 1686–1689.

[8] E. Lieb, R. Seiringer, J. Yngvason, Bosons in a trap: A rigorous derivation of the Gross-Pitaevskii energy functional, in: The Stability of Matter: From Atoms to Stars, Springer, 2001, pp. 685–697.

[9] A. Elgart, L. Erdős, B. Schlein, H.-T. Yau, Gross-Pitaevskii equation as the mean field limit of weakly coupled bosons, Archive for Rational Mechanics and Analysis 179 (2) (2006) 265–283.

[10] T. Bodurov, Derivation of the nonlinear Schrödinger equation from first principles, Annales de la Fondation Louis de Broglie 30 (3-4) (2005) 343–352.

[11] L. Salasnich, A. Parola, L. Reatto, Effective wave equations for the dynamics of cigar-shaped and disk-shaped Bose condensates, Physical Review A 65 (4) (2002) 043614.

[12] K. Mallory, R. A. Van Gorder, Stationary solutions for the 1+ 1 nonlinear Schrödinger equation modeling repulsive Bose-Einstein condensates in small potentials, Physical Review E 88 (1) (2013) 013205.

[13] K. Mallory, R. A. Van Gorder, Stationary solutions for the 1+ 1 nonlinear Schrödinger equation modeling attractive Bose-Einstein condensates in small potentials, Physical Review E 89 (1) (2014) 013204.

[14] K. Mallory, R. A. Van Gorder, Stationary solutions for the 2+ 1 nonlinear Schrödinger equation modeling Bose-Einstein condensates in radial potentials, Physical Review E 90 (2) (2014) 023201.

[15] K. Mallory, R. A. Van Gorder, Stationary solutions for the nonlinear Schrödinger equation modeling three-dimensional spherical Bose-Einstein condensates in general potentials, Physical Review E 92 (1) (2015) 013201.

[16] J. Bronski, L. Carr, B. Deconinck, J. Kutz, Bose-Einstein condensates in standing waves: The cubic nonlinear Schrödinger equation with a periodic potential, Physical Review Letters 86 (8) (2001) 1402.

[17] S. Theodorakis, E. Leontidis, Bound states in a nonlinear Kronig-Penney model, Journal of Physics A: Mathematical and General 30 (13) (1997) 4835.

[18] R. Carretero-González, D. Frantzeskakis, P. Kevrekidis, Nonlinear waves in Bose-Einstein condensates: Physical relevance and mathematical techniques, Nonlinearity 21 (7) (2008) R139.

[19] B. Malomed, Variational methods in nonlinear fiber optics and related fields, Progress in Optics 43 (2002) 71–194.

[20] V. Perez-Garcia, P. Torres, G. Montesinos, The method of moments for nonlinear Schrödinger equations: Theory and applications, SIAM Journal on Applied Mathematics 67 (4) (2007) 990–1015.

[21] P. Ghosh, Explosion-implosion duality in the Bose-Einstein condensation, Physics Letters A 308 (5) (2003) 411–416.

[22] Y. Kivshar, T. Alexander, S. Turitsyn, Nonlinear modes of a macroscopic quantum oscillator, Physics Letters A 278 (4) (2001) 225–230.

[23] T. Kapitula, P. Kevrekidis, B. Sandstede, Counting eigenvalues via the Krein signature in infinite-dimensional Hamiltonian systems, Physica D: Nonlinear Phenomena 195 (3) (2004) 263–282.

[24] Y. Kivshar, B. Malomed, Dynamics of solitons in nearly integrable systems, Reviews of Modern Physics 61 (4) (1989) 763.

[25] Q. D. Katatbeh, D. M. Christodoulou, New stationary solutions of the cubic nonlinear schrö dinger equations for bose-einstein condensates, arXiv preprint arXiv:1705.09721.

[26] P. Sandin, M. Ögren, M. Gulliksson, Numerical solution of the stationary multicomponent nonlinear schrödinger equation with a constraint on the angular momentum, Physical Review E 93 (3) (2016) 033301.

[27] Q. Xu, S. Song-He, L. Wei-Bin, Z. Hong, C. Xu-Dong, et al., A high-order conservative numerical method for gross–pitaevskii equation with time-varying coefficients in modeling bec, Chinese Phys. Lett 34 (2017) 060202.

[28] A. F. Biasi, J. Mas, A. Paredes, Delayed collapses of bose-einstein condensates in relation to anti-de sitter gravity, Physical Review E 95 (3) (2017) 032216.

[29] Z.-H. Zhang, S.-J. Yang, Exact periodic and solitonic states of the spinor condensates in a uniform external potential, Physica B: Condensed Matter 495 (2016) 82–88.

[30] A. Muryshev, G. Shlyapnikov, W. Ertmer, K. Sengstock, M. Lewenstein, Dynamics of dark solitons in elongated Bose-Einstein condensates, Physical Review Letters 89 (11) (2002) 110401.

[31] T. Köhler, Three-body problem in a dilute Bose-Einstein condensate, Physical Review Letters 89 (21) (2002) 210404.

[32] E. Kolomeisky, T. Newman, J. Straley, X. Qi, Low-dimensional Bose liquids: Beyond the Gross-Pitaevskii approximation, Physical Review Letters 85 (6) (2000) 1146.

[33] X.-Y. Tang, P. Shukla, Solution of the one-dimensional spatially inhomogeneous cubic-quintic nonlinear Schrödinger equation with an external potential, Physical Review A 76 (1) (2007) 013612.

[34] J. Belmonte-Beitia, J. Cuevas, Solitons for the cubic–quintic nonlinear Schrödinger equation with time- and space-modulated coefficients, Journal of Physics A: Mathematical and Theoretical 42 (16) (2009) 165201.

[35] J.-R. He, H.-M. Li, Analytical solitary-wave solutions of the generalized nonautonomous cubic-quintic nonlinear Schrödinger equation with different external potentials, Physical Review E 83 (6) (2011) 066607.

[36] C.-Q. Dai, D.-S. Wang, L.-L. Wang, J.-F. Zhang, W. Liu, Quasi-two-dimensional bose–einstein condensates with spatially modulated cubic–quintic nonlinearities, Annals of Physics 326 (9) (2011) 2356–2368.

[37] L. Gagnon, P. Winternitz, Exact solutions of the spherical quintic nonlinear Schrödinger equation, Physics Letters A 134 (5) (1989) 276–281.

[38] J. Belmonte-Beitia, G. Calvo, Exact solutions for the quintic nonlinear Schrödinger equation with time and space modulated nonlinearities and potentials, Physics Letters A 373 (4) (2009) 448–453.

[39] J. Belmonte-Beitia, V. Konotop, V. Pérez-García, V. Vekslerchik, Localized and periodic exact solutions to the nonlinear Schrödinger equation with spatially modulated parameters: Linear and nonlinear lattices, Chaos, Solitons & Fractals 41 (3) (2009) 1158–1166.

[40] B. Grébert, L. Thomann, Resonant dynamics for the quintic nonlinear Schrödinger equation, Annales de l'Institut Henri Poincare (C) Non Linear Analysis 29 (3) (2012) 455–477.

[41] L. Khaykovich, B. Malomed, Deviation from one dimensionality in stationary properties and collisional dynamics of matter-wave solitons, Physical Review A 74 (2) (2006) 023607.

[42] K. A. Theaker, R. A. Van Gorder, Hyper-Riccati equations and integrable reductions permitting stationary solutions for complex hyperbolic field equations, Applied Mathematics and Computation 219 (16) (2013) 8525–8541.

[43] V. Pérez-Garcıa, Self-similar solutions and collective coordinate methods for nonlinear Schrödinger equations, Physica D: Nonlinear Phenomena 191 (3) (2004) 211–218.

[44] L. Wen, L. Li, Z.-D. Li, S.-W. Song, X.-F. Zhang, W. Liu, Matter rogue wave in Bose-Einstein condensates with attractive atomic interaction, The European Physical Journal D-Atomic, Molecular, Optical and Plasma Physics 64 (2) (2011) 473–478.

[45] S. Adhikari, Numerical study of the spherically symmetric Gross-Pitaevskii equation in two space dimensions, Physical Review E 62 (2) (2000) 2937.

[46] W. Bao, D. Jaksch, P. Markowich, Numerical solution of the Gross-Pitaevskii equation for Bose-Einstein condensation, Journal of Computational Physics 187 (1) (2003) 318–342.

[47] F. K. Abdullaev, A. Gammal, L. Tomio, T. Frederico, Stability of trapped Bose-Einstein condensates, Physical Review A 63 (4) (2001) 043604.

[48] M. Landtman, Calculation of low lying states in the potential $V(r) = ar^2 + br^{-4} + cr^{-6}$ using B-spline basis sets, Physics Letters A 175 (3) (1993) 147–149.

[49] A. Fetter, Rotating vortex lattice in a Bose-Einstein condensate trapped in combined quadratic and quartic radial potentials, Physical Review A 64 (6) (2001) 063608.

[50] Y. Zhou, M. Karplus, K. Ball, R. Berry, The distance fluctuation criterion for melting: Comparison of square-well and Morse potential models for clusters and homopolymers, The Journal of Chemical Physics 116 (5) (2002) 2323–2329.

[51] Y.-X. Chen, Sech-type and Gaussian-type light bullet solutions to the generalized (3+ 1)-dimensional cubic-quintic Schrödinger equation in $\mathcal{PT}$-symmetric potentials, Nonlinear Dynamics 79 (1) (2015) 427–436.

[52] M. Greiner, I. Bloch, O. Mandel, T. Hänsch, T. Esslinger, Exploring phase coherence in a 2D lattice of Bose-Einstein condensates, Physical Review Letters 87 (16) (2001) 160405.

[53] M. Greiner, O. Mandel, T. Esslinger, T. Hänsch, I. Bloch, Quantum phase transition from a superfluid to a Mott insulator in a gas of ultracold atoms, Nature 415 (6867) (2002) 39–44.

[54] G. Chong, W. Hai, Q. Xie, Transient and stationary chaos of a Bose-Einstein condensate loaded into a moving optical lattice potential, Physical Review E 70 (3) (2004) 036213.

[55] Y. Shin, M. Saba, T. Pasquini, W. Ketterle, D. Pritchard, A. Leanhardt, Atom interferometry with Bose-Einstein condensates in a double-well potential, Physical Review Letters 92 (5) (2004) 050405.

[56] A. Smerzi, S. Fantoni, S. Giovanazzi, S. Shenoy, Quantum coherent atomic tunneling between two trapped Bose-Einstein condensates, Physical Review Letters 79 (25) (1997) 4950.

[57] K. W. Mahmud, H. Perry, W. Reinhardt, Quantum phase-space picture of Bose-Einstein condensates in a double well, Physical Review A 71 (2) (2005) 023615.

[58] F. Cataliotti, L. Fallani, F. Ferlaino, C. Fort, P. Maddaloni, M. Inguscio, Superfluid current disruption in a chain of weakly coupled Bose-Einstein condensates, New Journal of Physics 5 (1) (2003) 71.

[59] K. Law, P. Kevrekidis, B. Anderson, R. Carretero-González, D. Frantzeskakis, Structure and stability of two-dimensional Bose-Einstein

condensates under both harmonic and lattice confinement, Journal of Physics B: Atomic, Molecular and Optical Physics 41 (19) (2008) 195303.

[60] C. Xiong, M. R. R. Good, Y. Guo, X. Liu, K. Huang, Relativistic superfluidity and vorticity from the nonlinear klein-gordon equation, Physical Review D 90 (12) (2014) 125019.

[61] M. I. Weinstein, Lyapunov stability of ground states of nonlinear dispersive evolution equations, Communications on Pure and Applied Mathematics 39 (1) (1986) 51–67.

[62] P. Gérard, Z. Zhang, Orbital stability of traveling waves for the one-dimensional gross–pitaevskii equation, Journal de mathématiques pures et appliquées 91 (2) (2009) 178–210.

[63] R. A. Van Gorder, Orbital instability of the peregrine soliton, Journal of the Physical Society of Japan 83 (5) (2014) 054005.

[64] T. Gallay, D. Pelinovsky, Orbital stability in the cubic defocusing nls equation: I. cnoidal periodic waves, Journal of Differential Equations 258 (10) (2015) 3607–3638.